AD-A186 901 ENERGY DISTRIBUTION OF CERENKOV RADIATION FOR FINITE FREQUENCY INTERVALS(U) NAVAL POSTGRADUATE SCHOOL MONTEREY CA T M WILBUR JUN 87 1/1

UNCLASSIFIED F/G 20/8 NL

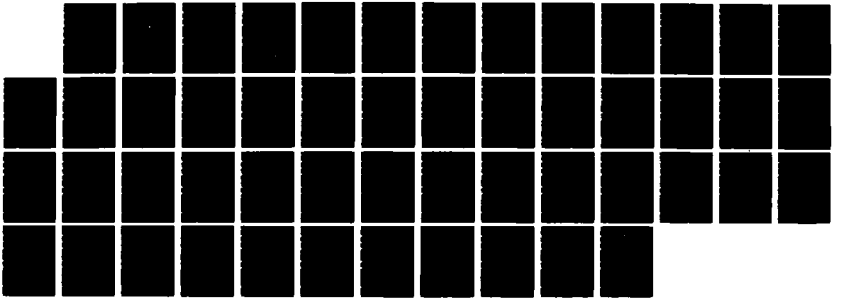

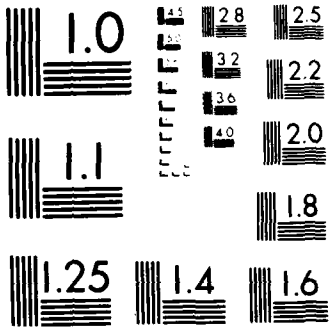

NAVAL POSTGRADUATE SCHOOL
Monterey, California

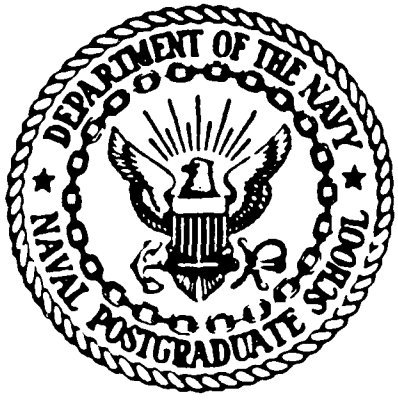

THESIS

ENERGY DISTRIBUTION OF CERENKOV
RADIATION
FOR
FINITE FREQUENCY INTERVALS

by

Thomas M. Wilbur

June 1987

Thesis Advisor J.R. Neighbours

SECURITY CLASSIFICATION OF THIS PAGE

REPORT DOCUMENTATION PAGE

1a REPORT SECURITY CLASSIFICATION UNCLASSIFIED	1b RESTRICTIVE MARKINGS
2a SECURITY CLASSIFICATION AUTHORITY	3 DISTRIBUTION/AVAILABILITY OF REPORT Approved for public release; distribution is unlimited
2b DECLASSIFICATION/DOWNGRADING SCHEDULE	
4 PERFORMING ORGANIZATION REPORT NUMBER(S)	5 MONITORING ORGANIZATION REPORT NUMBER(S)
6a NAME OF PERFORMING ORGANIZATION Naval Postgraduate School	6b OFFICE SYMBOL (If applicable) 61
7a NAME OF MONITORING ORGANIZATION Naval Postgraduate School	
6c ADDRESS (City, State, and ZIP Code) Monterey, California 93943-5000	7b ADDRESS (City, State, and ZIP Code) Monterey, California 93943-5000
8a NAME OF FUNDING/SPONSORING ORGANIZATION	8b OFFICE SYMBOL (If applicable)
8c ADDRESS (City, State, and ZIP Code)	9 PROCUREMENT INSTRUMENT IDENTIFICATION NUMBER
	10 SOURCE OF FUNDING NUMBERS PROGRAM ELEMENT NO / PROJECT NO / TASK NO / WORK UNIT ACCESSION NO

11 TITLE (Include Security Classification)
ENERGY DISTRIBUTION OF CERENKOV RADIATION FOR FINITE FREQUENCY INTERVALS

12 PERSONAL AUTHOR(S)
Wilbur, Thomas M.

13a TYPE OF REPORT	13b TIME COVERED FROM ___ TO ___	14 DATE OF REPORT (Year Month Day)	15 PAGE COUNT
Master's Thesis		1987 June	50

16 SUPPLEMENTARY NOTATION

17 COSATI CODES			18 SUBJECT TERMS (Continue on reverse if necessary and identify by block number)
FIELD	GROUP	SUB GROUP	Cerenkov radiation, Electron Accelerator

19 ABSTRACT (Continue on reverse if necessary and identify by block number)

The equation defining the energy radiated per unit solid angle due to Cerenkov radiation is analyzed in detail, including the effects of all equation variables for a hypothetical electron accelerator experiment. Specifically, various finite frequency intervals are used in an effort to determine the optimum means of determining the details of a charge bunch in a high energy electron accelerator. In particular, it is shown how narrowband measurements as a function of angle may yield information on both the beam path length and the bunch charge parameters. As an aid to the analysis, an interactive Fortran program is presented that allows for any specific experimental parameters, with options for various output types as desired.

20 DISTRIBUTION/AVAILABILITY OF ABSTRACT	21 ABSTRACT SECURITY CLASSIFICATION
☒ UNCLASSIFIED/UNLIMITED ☐ SAME AS RPT ☐ DTIC USERS	UNCLASSIFIED
22a NAME OF RESPONSIBLE INDIVIDUAL J. R. Neighbours	22b TELEPHONE (Include Area Code) (408) 646-2291 / 22c OFFICE SYMBOL 61Nb

DD FORM 1473, 84 MAR 83 APR edition may be used until exhausted
All other editions are obsolete

SECURITY CLASSIFICATION OF THIS PAGE

Approved for public release; distribution is unlimited.

Energy Distribution of Cerenkov Radiation
for
Finite Frequency Intervals

by

Thomas M. Wilbur
Lieutenant, United States Navy
B.S., Pennsylvania State University, 1978.

Submitted in partial fulfillment of the
requirements for the degree of

MASTER OF SCIENCE IN PHYSICS

from the

NAVAL POSTGRADUATE SCHOOL
June 1987

Author: _____
Thomas M. Wilbur

Approved by: _____
J.R. Neighbours, Thesis Advisor

_____
F.R. Buskirk, Second Reader

_____
K.E. Woehler, Chairman,
Department of Physics

_____
Gordon E. Schacher,
Dean of Science and Engineering

ABSTRACT

The equation defining the energy radiated per unit solid angle due to Cerenkov radiation is analyzed in detail, including the effects of all equation variables for a hypothetical electron accelerator experiment. Specifically, various finite frequency intervals are used in an effort to determine the optimum means of determining the details of a charge bunch in a high energy electron accelerator. In particular, it is shown how narrowband measurements as a function of angle may yield information on both the beam path length and the bunch charge parameters. As an aid to the analysis, an interactive Fortran program is presented that allows for any specific experimental parameters, with options for various output types as desired.

THESIS DISCLAIMER

The reader is cautioned that computer programs developed in this research may not have been exercised for all cases of interest. While every effort has been made, within the time available, to ensure that the programs are free of computational and logic errors, they cannot be considered validated. Any application of these programs without additional verification is at the risk of the user.

TABLE OF CONTENTS

LIST OF TABLES

LIST OF FIGURES

ACKNOWLEDGEMENTS

The author gratefully acknowledges Professors J.R. Neighbours and F.R. Buskirk for their direction and guidance in preparing this thesis.

I. INTRODUCTION

A. HISTORY

The existence of the phenomenon now known as Cerenkov radiation was observed as early as 1910, most notably by Madam Curie. However, during the ensuing years, there was other work being completed by those familiar with Madam Curie's observation that masked a detailed study of the phenomenon. Jelley [Ref. 1] explains their reasons in greater detail. In 1926, Mallet made the first deliberate attempt to study and explain "the very faint emission of a bluish-white light from transparent substances". Experimentation concerning this phenomenon continued through the 1920's and 1930's by Cerenkov and Mallet, but a viable theory explaining the process would not be proposed until 1937 by Frank and Tamm. Their theory, for which they were consequently awarded the 1958 Nobel Prize in Physics, was found to be in excellent agreement with the experimental results obtained by Cerenkov. The advent of more sensitive light detectors and other experimental equipment accounted for more in depth studies of Cerenkov radiation in the 1940's and 1950's. [Ref. 1: pp. 1-8]

Since then, numerous experiments have been conducted and many papers and academic theses published that have helped to more clearly understand and explain the Cerenkov radiation phenomenon. Some of the more recent investigations include; periodic electron bunches of finite emission lengths, time developement of bunch charges and Cerenkov radiation in the x-ray region, (see Bibliography).

B. BACKGROUND

Work on this thesis was motivated by two factors. First, using previously derived equations and expressions describing the energy radiated per unit solid angle due to Cerenkov radiation, [Ref. 2] a fortran program was written to run on the IBM 3033 mainframe. The program, (see Appendix), was written interactively to allow all parameters to be changed in order to tailor the output to fit any specific experimental setup.

Second, using the aforementioned Fortran program, a series of outputs were generated to be used in comparing the theoretical results of previously derived expressions with those of actual experimentation. Since there are literally an infinite

number of combinations of various parameters, only a few were chosen to be included in this work. The parameters chosen are consistent with those expected while conducting experiments on any high energy electron accelerator.

II. THEORY

A. CERENKOV EFFECT

Cerenkov radiation can most easily be explained by describing the interaction of a single electron within a transparent medium. Consider a non-relativistic electron. While traversing the medium, the electron will tend to locally polarize the adjacent atoms in the medium, instantaneously creating a temporary dipole within the material. Therefore, as the electron moves through the medium, an electromagnetic pulse is generated. However, since there is complete symmetry, there will be no net field generated. See Figure 2.1.

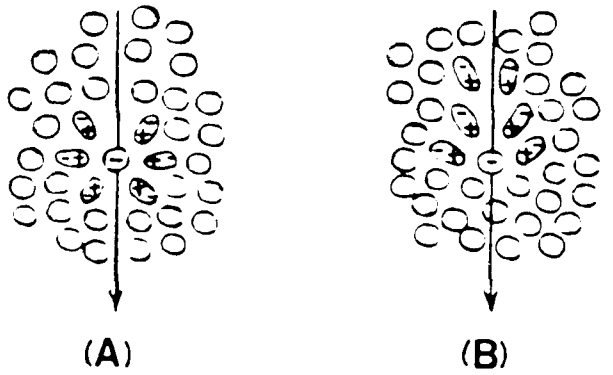

Figure 2.1 Polarized Atoms in a Dielectric.

Now suppose an electron is travelling at a speed comparable to or exceeding the speed of light for the medium. Although symmetry is preserved in the azimuthal plane, along the axis of motion a resultant dipole field is generated. These fields are set up at each element along the electron's track, radiating a brief electromagnetic pulse. Provided the electron is moving at a speed greater than the speed of light within the medium, the wavelets formed from all elemental positions on the track can be in phase and thus produce a resultant electromagnetic field. [Ref. 1: pp 3-6]

Figure 2.2 depicts the relationship of the distance (BZ) travelled by an electron in time Δt versus the distance (BA) covered by an emitted electromagnetic pulse during the same time. The distance (BZ) travelled by the electron is given by:

$$BZ = \beta c_0 \Delta t, \qquad \text{(eqn 2.1)}$$

where β is the ratio of the electron speed to the speed of light in a vacuum ,c_0. The distance (*B.1*) travelled by the electromagnetic wave is given by:

$$BA = c\Delta t, \qquad \text{(eqn 2.2)}$$

where c is the speed of light for the medium. For a medium with an index of refraction n, $c = c_0/n$. From equations 2.1 and 2.2, the "cerenkov relation" is obtained. [Ref. 1: pp 6-8]

$$\cos\theta_c = 1/\beta n. \qquad \text{(eqn 2.3)}$$

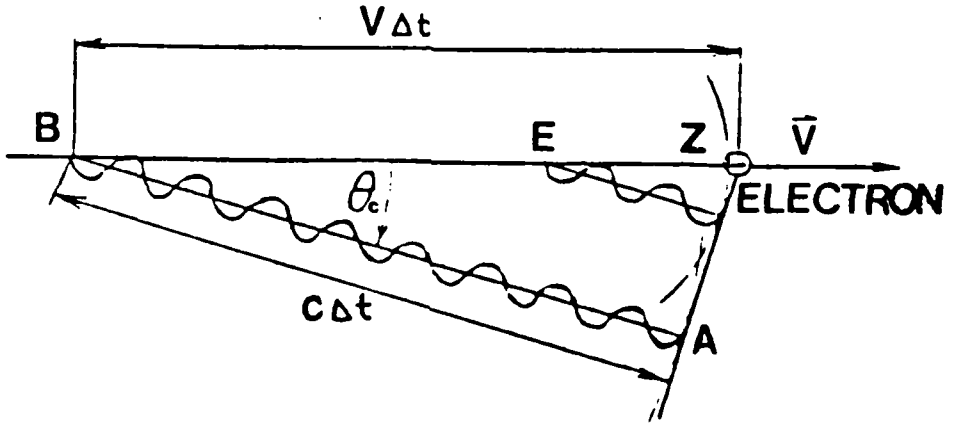

Figure 2.2 Illustration of Cerenkov Radiation.

Due to the finite path length at which the radiation is detected, the Cerenkov cone angle is normally shifted away from θ_c. As the frequency at which the emitted radiation is measured or the distance from the source is increased, the radiation cone angle approaches θ_c. As this occurs, an increasing fraction of the total Cerenkov radiation is found at θ_c. [Ref. 2]

B. MATHEMATICAL INTERPRETATION

1. Energy Equation

As previously discussed, for a finite path length, diffracted Cerenkov radiation effects will be seen at angles other than the Cerenkov angle. Previous work on this phenomenon [Ref. 2] has resulted in an expression for the emitted Cerenkov radiation. The energy radiated per unit solid angle within the frequency range dν by a single bunch charge q travelling a finite distance L is:

$$E(\nu,k)d\nu = QR^2d\nu, \qquad \text{(eqn 2.4)}$$

where Q is a constant whose magnitude is dependent on the index of refraction and the total charge in Coulombs.

$$Q = \mu cq^2/8\pi^2. \qquad \text{(eqn 2.5)}$$

The radiation function R is given by:

$$R = 2\pi\eta\sin\theta I(u)F(k), \qquad \text{(eqn 2.6)}$$

where θ is the angle measured from the line of travel of the bunch charge to the direction of propagation of the emitted radiation, I(u) is the diffraction function, and $F(k)$ is a form factor. For convenience, the length of travel of the bunch charge is measured in units of the wavelength of the emitted radiation within the medium. The dimensionless beam length parameter η serves this purpose and is defined as the ratio of the length L from the source to the wavelength λ of the emitted radiation.

$$\eta = L/\lambda. \qquad \text{(eqn 2.7)}$$

The diffraction function is defined as:

$$I(u) = \sin(u)/u, \qquad \text{(eqn 2.8)}$$

where u is dependent on both the angle θ and the beam length parameter η.

$$u = \pi\eta\{(1/n\beta) - \cos\theta\}. \qquad \text{(eqn 2.9)}$$

Equations 2.5 through 2.9 can then be used to redefine equation 2.4 in terms of experimental constants, (i.e. n, L, β etc.) and the single remaining variable of frequency. [Ref. 2]

$$E(\nu,k)d\nu = QG^2F^2(k)\sin^2\{A\nu\}d\nu. \qquad \text{(eqn 2.10)}$$

For a given experimental setup, A and G are functions of the angle only and are defined as follows:

$$A = \{L\pi/c\}\bullet\{(1/n\beta)-\cos\theta\}, \text{ and} \qquad \text{(eqn 2.11)}$$

$$G = \{2\sin\theta\}/\{(1/n\beta)-\cos\theta\}. \qquad \text{(eqn 2.12)}$$

The radiation patterns arising from equation 2.4 can be thought of as an oscillating $\sin^2 x$ function modulated by an envelope. If $F(k)$ is neglected, then G^2 acts as the modulating envelope. The actual form of the envelope will vary with $n\beta$, but will be constant for a given experimental setup. Figure 2.3 shows a plot of G^2 as an illustrative example for values of $n\beta$ two percent above and below threshold, ($n\beta = 1.0 \pm 0.02$).

Finally, the dimensionless form factor $F(k)$ is related to the Fourier transform of the bunch charge distribution. The Fourier components of any bunch charge are defined as:

$$\rho(k) = \int\rho(r)e^{ik\cdot r}d^3r, \qquad \text{(eqn 2.13)}$$

where $\rho(r)$ defines the charge distribution of the bunch charge. Once the Fourier components are determined from equation 2.13, the form factor is found by the relation:

$$\rho(k) = qF(k). \qquad \text{(eqn 2.14)}$$

Here we consider only a line charge with distribution $\rho(z)$ which is travelling in the z direction. Thus, $r \rightarrow z$ in equation 2.13 and $k \rightarrow k_z$ in equation 2.14. In this work, only

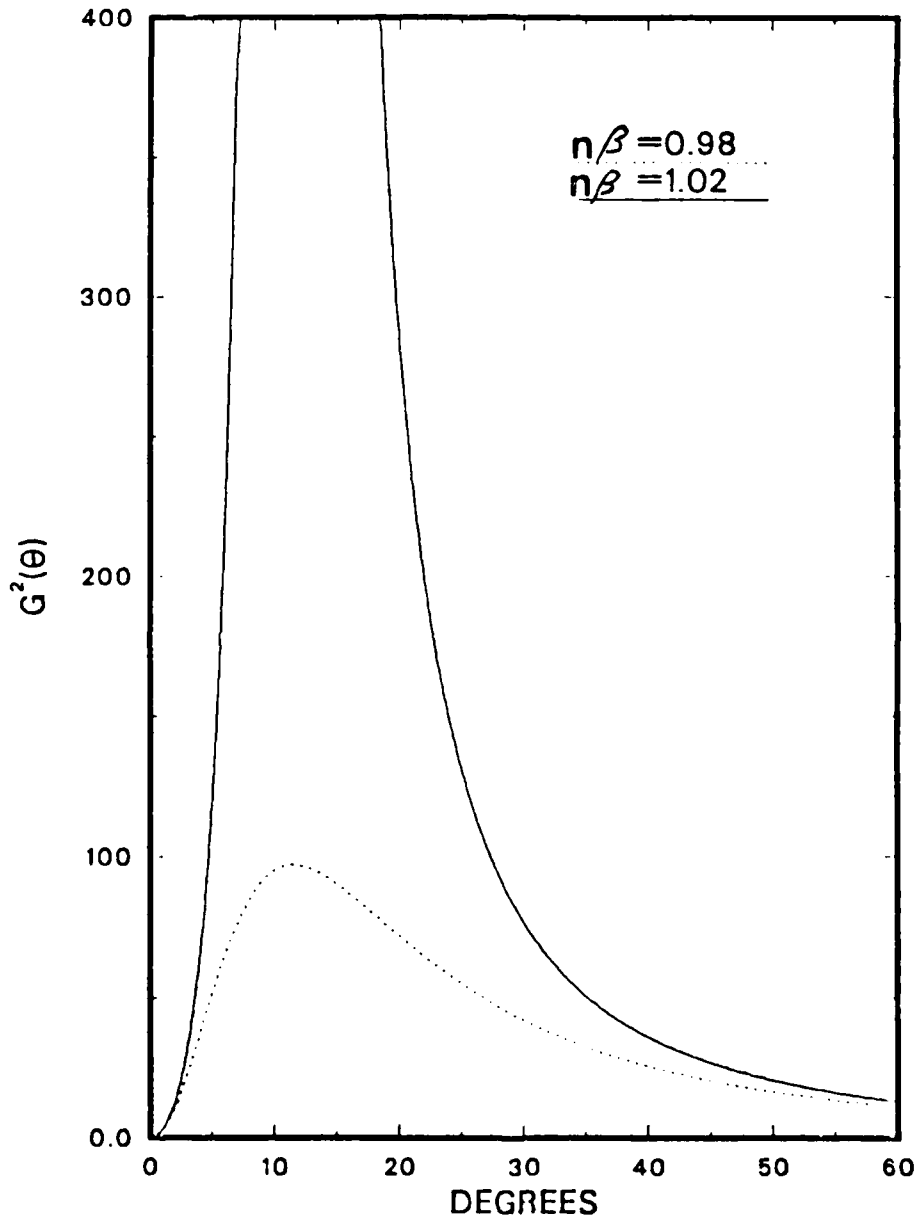

Figure 2.3 Illustrative Example of the Cerenkov Radiation Envelope.

the trapezoidal bunch charge distribution is used although many others are available and easily used within the Fortran program. [Ref. 3]

2. **Trapezoidal Form Factor**

The first step in obtaining any type of form factor is to determine the assumed geometry of the emitted bunch charge. Figure 2.4 depicts the geometry for the trapezoidal bunch charge. The functions defining the positive half of the trapezoid are given by:

$$f_1(x) = A, \text{ and} \qquad \text{(eqn 2.15)}$$

$$f_2(x) = \{A/(d-b)\} \bullet \{d-x\}, \qquad \text{(eqn 2.16)}$$

where f_1 defines the trapezoid from 0 to b and f_2 defines the trapezoid from b to d. The amplitude of the bunch charge is denoted as A with units of coulombs per meter. The values b and d have units of meters and are easily obtained from the pulse length.

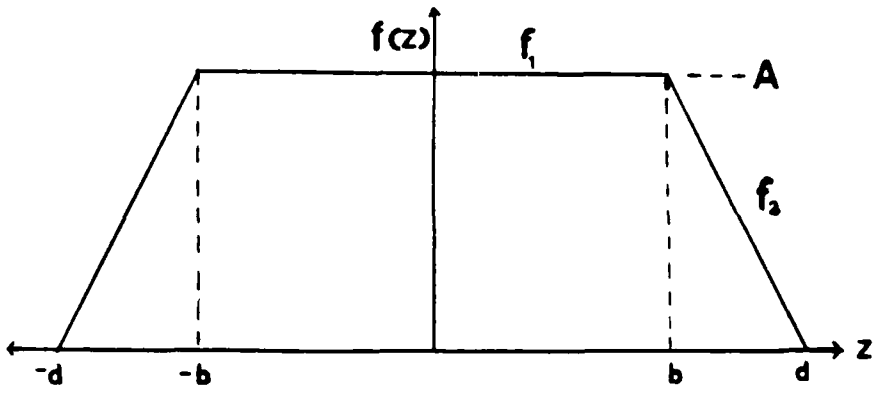

Figure 2.4 Trapezoidal Bunch Charge.

The fourier components of this trapezoid are defined by equation 2.13 where $\rho(k_z)$ is the sum of the two functions $f_1(x)$ and$f_2(x)$, (ie. the charge distribution of a single bunch charge), and k_z is the component of the wave vector k. The details of solving equation 2.13, though tedious, are rather straightforward. [Ref. 3]

Equation 2.17 is the solution to equation 2.13 and provides the Fourier components in the case of the trapezoid.

$$\rho(k_z) = \{ (2A)(d-b)/k^2_z \} \bullet \{ \cos(k_z b) - \cos(k_z d) \}. \qquad \text{(eqn 2.17)}$$

The value of A is found by equating q, the total bunch charge, to the integral of the charge distribution.

$$q = \int_{-\infty}^{\infty} \rho(z)dz = A(b+d). \qquad \text{(eqn 2.18)}$$

By substituting the results of equations 2.17 and 2.18 into equation 2.14, the form factor for the trapezoidal charge distribution is:

$$F(k_z) = \{ 2q/(d^2-b^2) \} \bullet \{1/k^2\} \bullet \{ \cos(k_z b)-\cos(k_z d) \}. \qquad \text{(eqn 2.19)}$$

If the medium is assumed to be non-dispersive, then $\omega = ck_z$ and remembering that $k_z = k\cos\theta$, the form factor can be written in terms of the angular frequency $2\pi\nu = \omega$. After substituting, the explicit relation for the trapezoidal form factor is given by equation 2.20 as follows:

$$F(k_z) = \{ c^2/2\pi^2(d^2-b^2) \} \bullet \{ \cos(B\nu)-\cos(D\nu) \} \bullet \{ 1/\nu^2 \}, \qquad \text{(eqn 2.20)}$$

where B and D are given by equations 2.21 and 2.22 respectively.

$$B = 2\pi b\cos\theta/c, \text{ and} \qquad \text{(eqn 2.21)}$$

$$D = 2\pi d\cos\theta/c. \qquad \text{(eqn 2.22)}$$

It is clearly seen that once the parameters for the bunch charge are defined, the form factor is highly dependent on the inverse square of the frequency ν. The expression for the energy radiated per unit solid angle within the frequency range $d\nu$ written in terms of frequency will then be equation 2.4 with the form factor as given in equation 2.20. [Ref. 4]

$$Edv = [\ QG^2\sin^2(Av)\ ] \qquad \text{(eqn 2.23)}$$
$$\bullet[\ \{c^2/2\pi^2(d^2-b^2)\}\{\cos(Bv)-\cos(Dv)\}\ \{1/v^2\}\ ]^2dv.$$

The radiated energy is a function of frequency through both the $\sin^2(Av)$ term and the form factor.

III. RESULTS AND ANALYSIS

The Fortran program written for this work has various output capabilities. The first type of output contains data equating the explicit value of E (eqn.2.4), in joule-seconds, to a specific frequency at a particular angle θ. Another output type provides data for graphing the radiation envelope (eqn.2.3) or the form factor (eqn. 2.20) used in this thesis. These graphs are useful in understanding the complex nature of the variables involved in solving equation 2.4.

The most useful output type is that which solves, (i.e. integrates), equation 2.4 over a predetermined frequency range for all desired angles from the beam path. A careful study of these graphical outputs will provide insight into the particulars necessary for any experimental setup so that the most accurate and informative results can be obtained.

As previously discussed, the output obtained during this work are based on a set of parameters that uniquely define a specific electron accelerator experimental setup. The following input parameters (with their Fortran variable names), are required:

1. Accelerator Beam Energy (EBEAM).
2. Total Periodic Electron Bunch Charge (CUE).
3. Index of Refraction (IND).
4. Distance from Source to Detector (LENGTH).
5. Cerenkov Radiation Frequency Interval (MIDNU,ENU).
6. Incremental Change in Frequency Interval (DNU).
7. Angle of Interest, as Measured from the Charge Path (DTHETA).
8. Bunch Charge Form Factor (FORFAC).
9. Trapezoidal Bunch Parameters (BEE,DEE).

The specific values for each variable used to obtain the outputs in this work are as follows:

1. Beam Energy - 50 MEV.
2. Bunch Charge - .001 Coulombs.
3. Index of Refraction - 1.000268 (air).
4. Source to Detector Distance - 100 Meters.
5. Frequency Interval - As noted.
6. Frequency Increment - 0.5 MHz.

7. Solid Angle - As noted.
8. Form Factor - Unity and Trapezoid.
9. Trapezoidal Bunch Parameters.
    a. Top-50 nanoseconds.
    b. Base-60 nanoseconds.

For the given index of refraction and beam energy, the "Cerenkov Relation" (eqn.2.3) gives the critical Cerenkov angle as 1.9°.

Three basic assumptions were made in the course of this work. First, it is assumed that the shape of the trapezoidal bunch charge remains unchanged as it travels through the medium. This is reasonable since the distances involved are relatively short with respect to the speed at which the bunch charge is travelling. Second, the permeability of free space μ is used vice that of the actual medium of air.

The final assumption is that the speed of the electron bunch remains unchanged throughout it's travel. Although there is some Bremstrahlung radiation emitted, it has a negligeable effect on the speed of the bunch charge and therefore β is assumed to remain constant.

Figure 3.1 depicts the energy radiated per unit frequency at angles of 30, 45 and 60 degrees using a form factor of unity. As would be expected from equation 2.23, a $\sin^2 x$ function results since Q (eqn.2.5), A(eqn.2.11) and G(eqn.2.12) are all constant at the given angle θ, the only variable being the frequency ν. The difference in amplitudes is due to the variation of G with θ. The difference in the periods is due to the function A, which, as the argument of the sin term, effects the periodicity.

Once a form factor other than unity is used, the output pattern is changed significantly. Equation 2.23 shows the frequency dependence of the trapezoidal form factor. Figure 3.2 is the form factor obtained at 0 degrees over the frequency range 10-100 MHz. The damping of the form factor waveform is due to the inverse square relationship of $F(k)$ with frequency. Figures 3.3 and 3.4 depict the square of the form factor as it is used in equation 2.4. Different frequency intervals are used but each waveform is computed at the same angle, $\theta = 0°$. As with Figure 3.2, Figures 3.3 and 3.4 each dampen with increasing frequency. The increased periodicity of Figure 3.4 is due primarily to the wider frequency range. At angles other than $\theta = 0°$ the form factor will be similar in shape except scaled by changes in B and D due to the $\cos\theta$ factor. [Ref. 4]

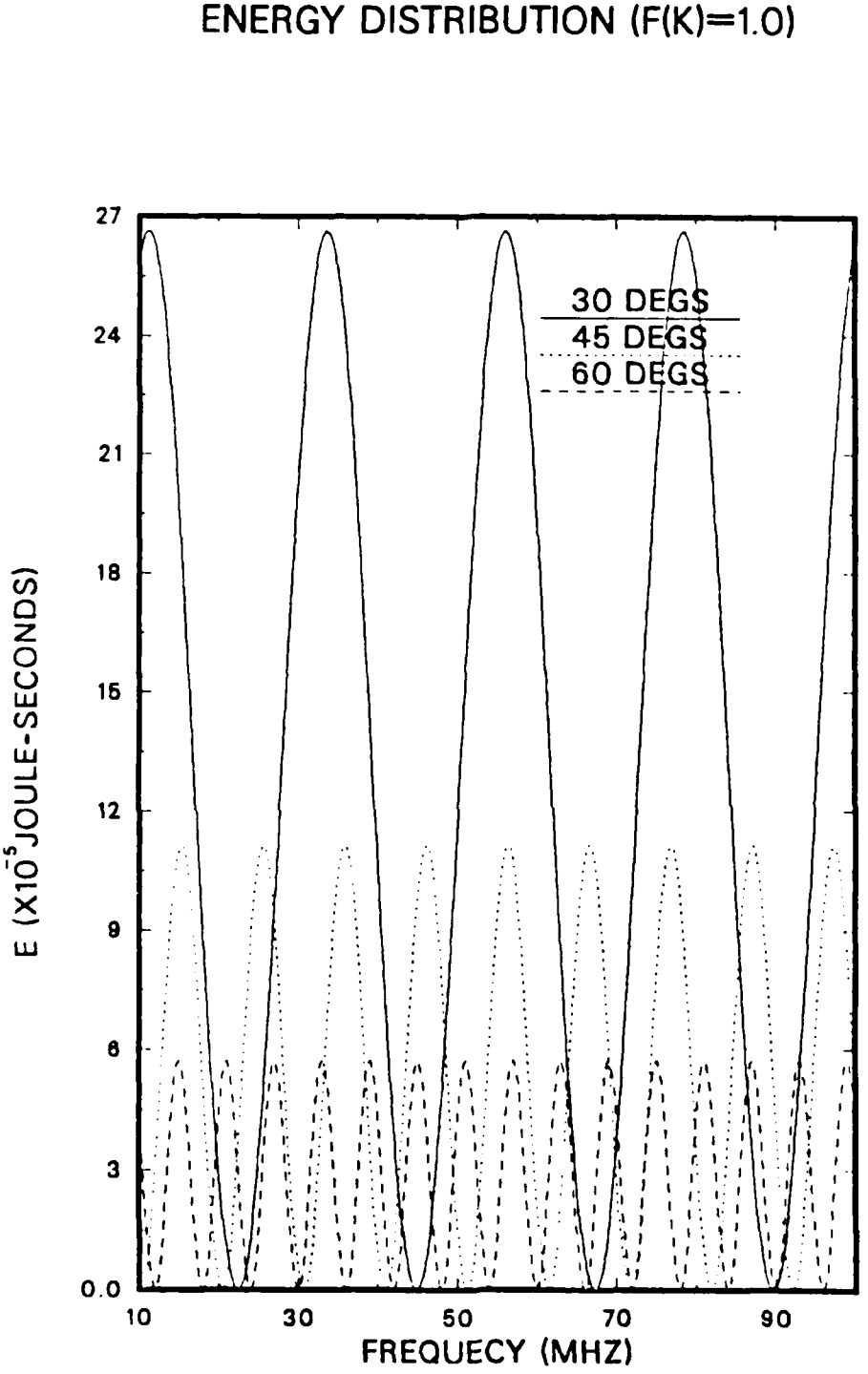

Figure 3.1 Energy Radiated per Unit Frequency, (θ = 30°,45° and 60°).

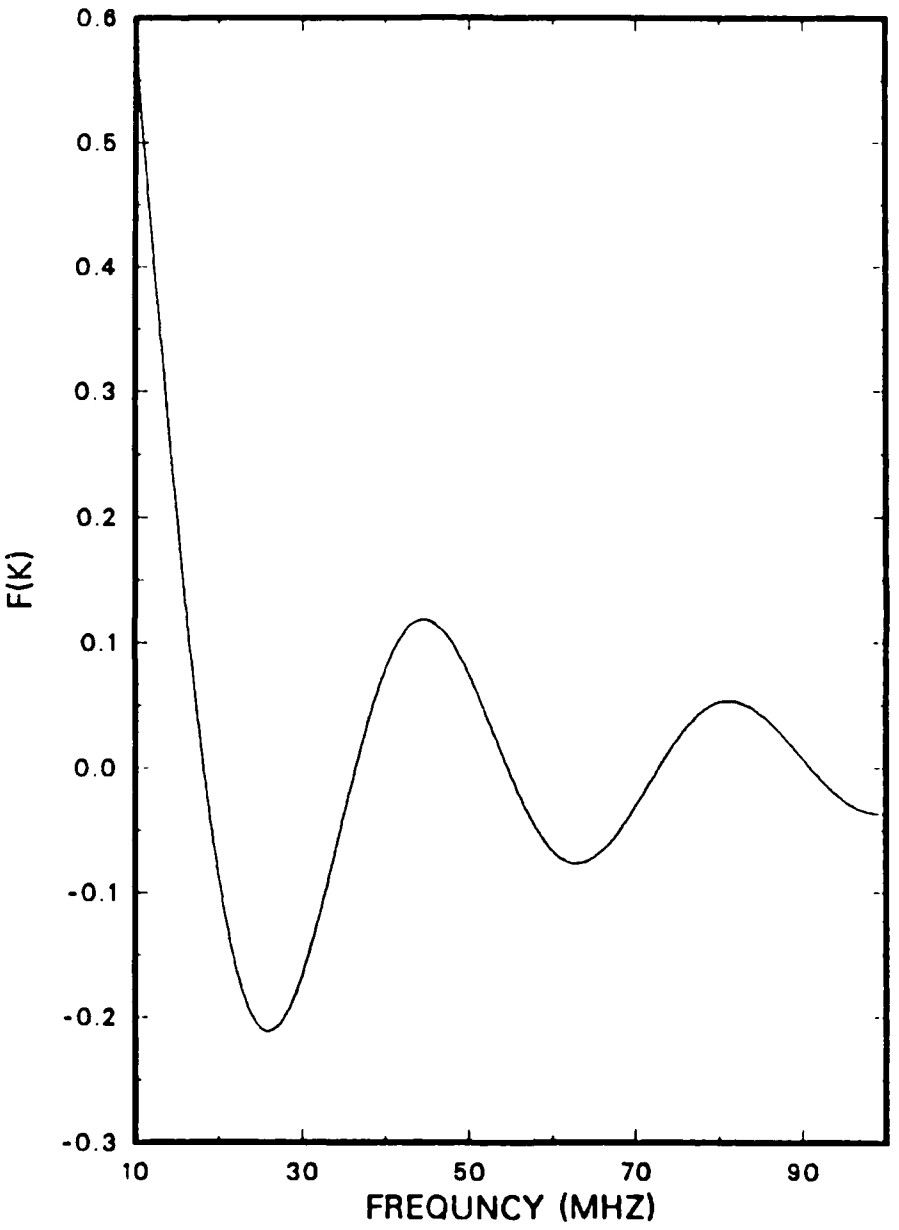

Figure 3.2 Trapezoidal Form Factor, ($\theta = 0^{o}$).

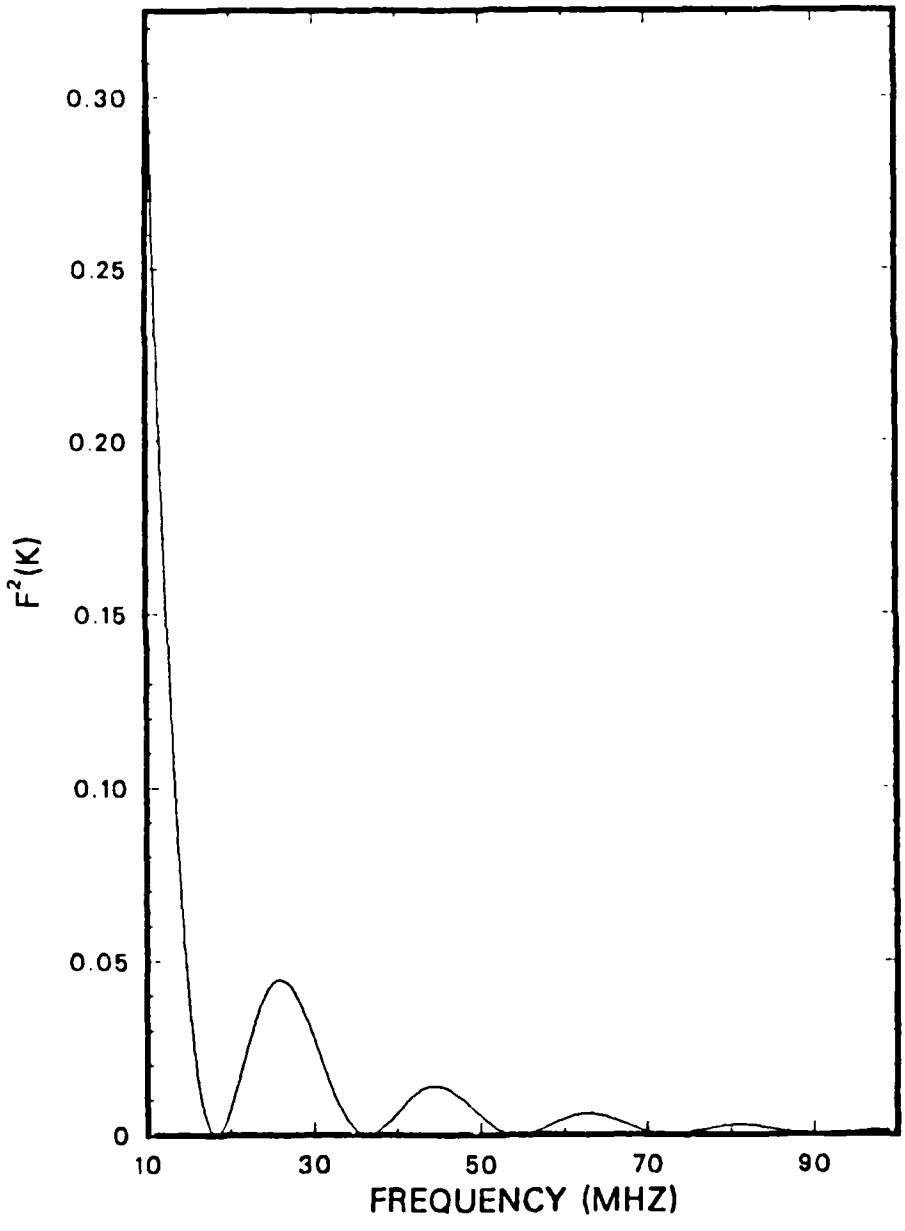

Figure 3.3 Square of the Trapezoidal Form Factor, 10-100MHz., (θ = 0°).

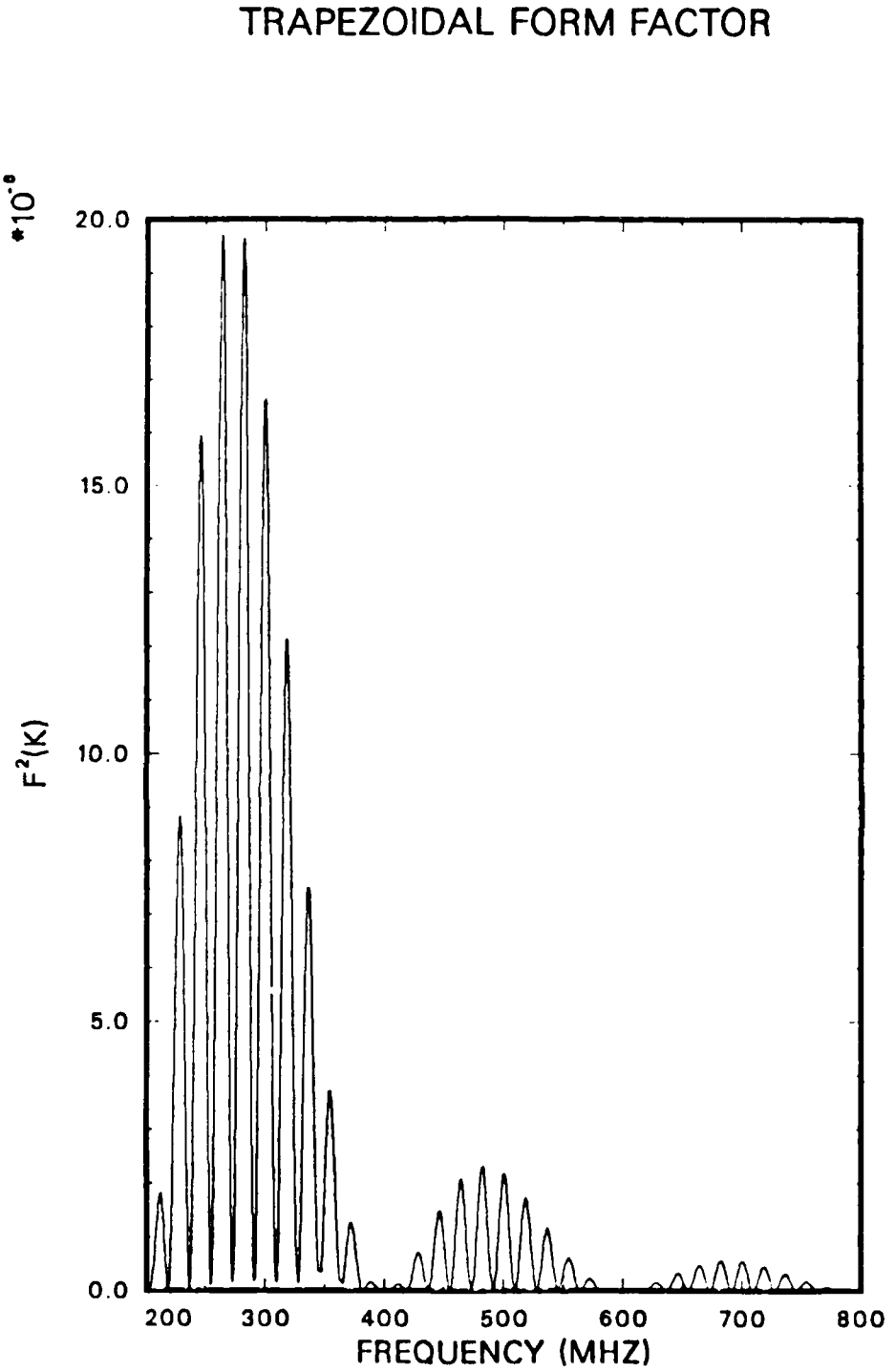

Figure 3.4 Square of the Trapezoidal Form Factor, 200-800MHz., (θ = 0°).

Figure 3.5 is a plot similar to that of Figure 3.1 except that the unity form factor has been replaced with that of the trapezoid. As expected, the use of a specific form factor significantly effects the output. The output of interest will be the integration of all outputs similar to Figure 3.5 at each angle of interest. Before analyzing the integrated output with the trapezoidal form factor, it is useful to look at Figures 3.6 through 3.8 which depict the integration of equation 2.23 while maintaining unity form factor. As noted earlier, an energy peak at the Cerenkov angle of 1.9° is expected. Although the peak appears to be centered at about 10° in Figure 3.6, as the frequency interval increases from 10-100 MHz. to 10-10,000 MHz. the same curve shifts closer to the Cerenkov angle. Concurrently, the graphs become smoother as more data points are used at each interval θ. The aberration found in Figure 3.8 may be an artifact of the Fortran program. The extraordinarily large magnitude of Figure 3.8 is due to the existence of a pole in variable G (eqn.2.12) of equation 2.10 as θ approaches the critical Cerenkov angle. However, since the variable A is zero at the Cerenkov Angle, equation 2.10 remains finite. [Ref. 2]

Figure 3.9 shows the output of equation 2.23 integrated over a relatively broadband frequency range of 100 to 1,000 MHz. Figure 3.10 is the identical output plotted over a narrower range of θ to enhance the output detail. In each case, the detail of the output is fuzzy at best, making it difficult to conduct any meaningful analysis. In an attempt to force more detail in the output, the frequency range over which equation 2.23 is integrated was narrowed. Figure 3.11 depicts the energy spectra integrated over 20 MHz. centered around 100 MHz. All other parameters are equal to those used in Figures 3.9 and 3.10. Although similar in general form , Figure 3.11 shows more detail. Then, changing to a narrower frequency band of 2 MHz.(again centered around 100 MHz.), Figure 3.12 depicts a clearly defined output that is similar to a frequency modulated carrier wave. Figure 3.13 shows the same output for a narrower range of θ to show more detail.

The Cerenkov radiation envelope discussed earlier(Figure 2.3) has an impact on the outputs of Figures 3.12 and 3.13, but once $n\beta$ is selected the envelope will effect only the amplitude of this and similar graphs. The null points of Figures 3.12 and 3.13 can then be calculated by analyzing the components of the radiation function(eqn.2.6). The expression for the trapezoidal bunch charge form factor(eqn.2.20) can be expressed as a product of a constant and two sin functions using the following trigonometric identity.

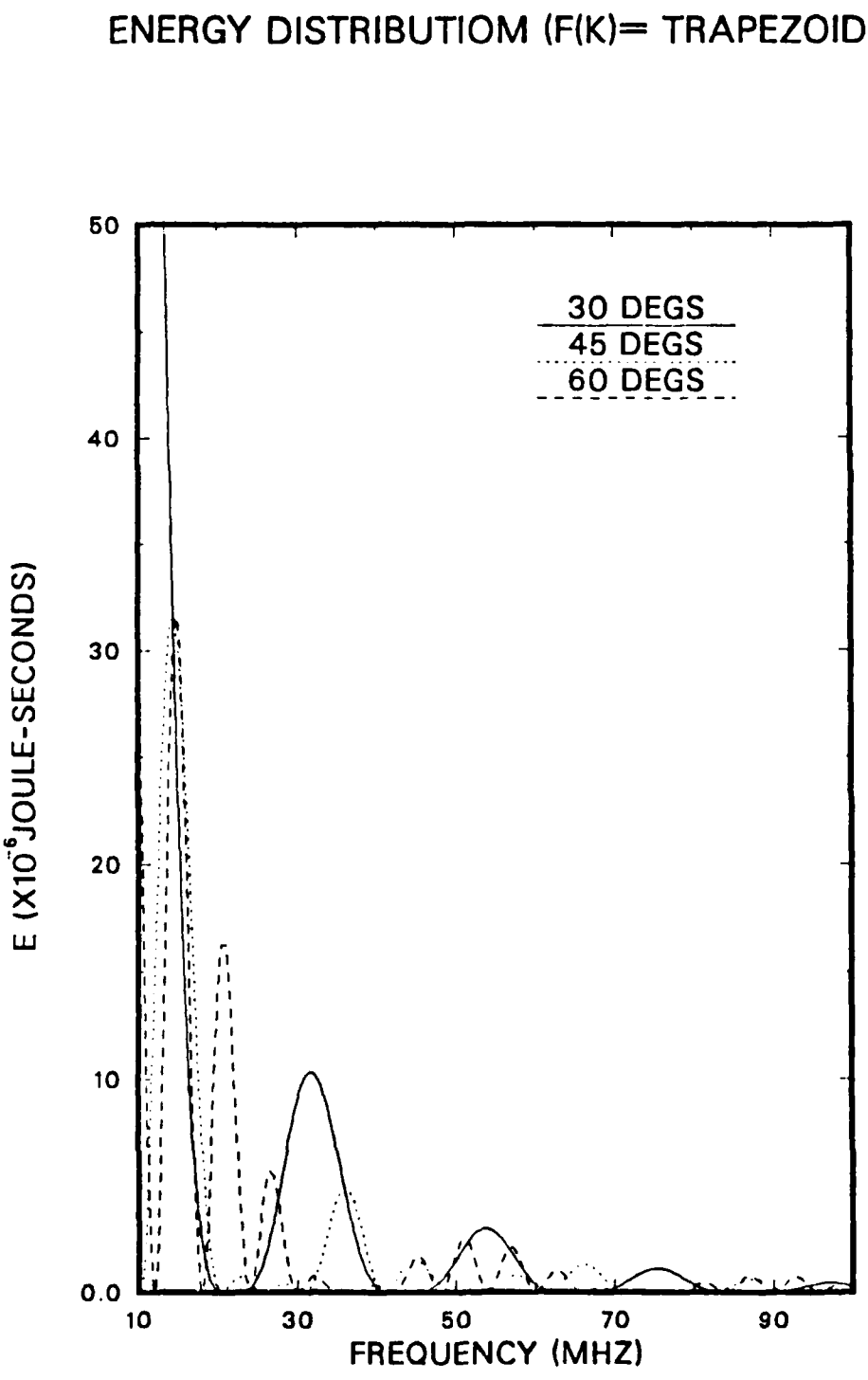

Figure 3.5 Energy Radiated per Unit Frequency, (θ = 30°, 45° and60°).

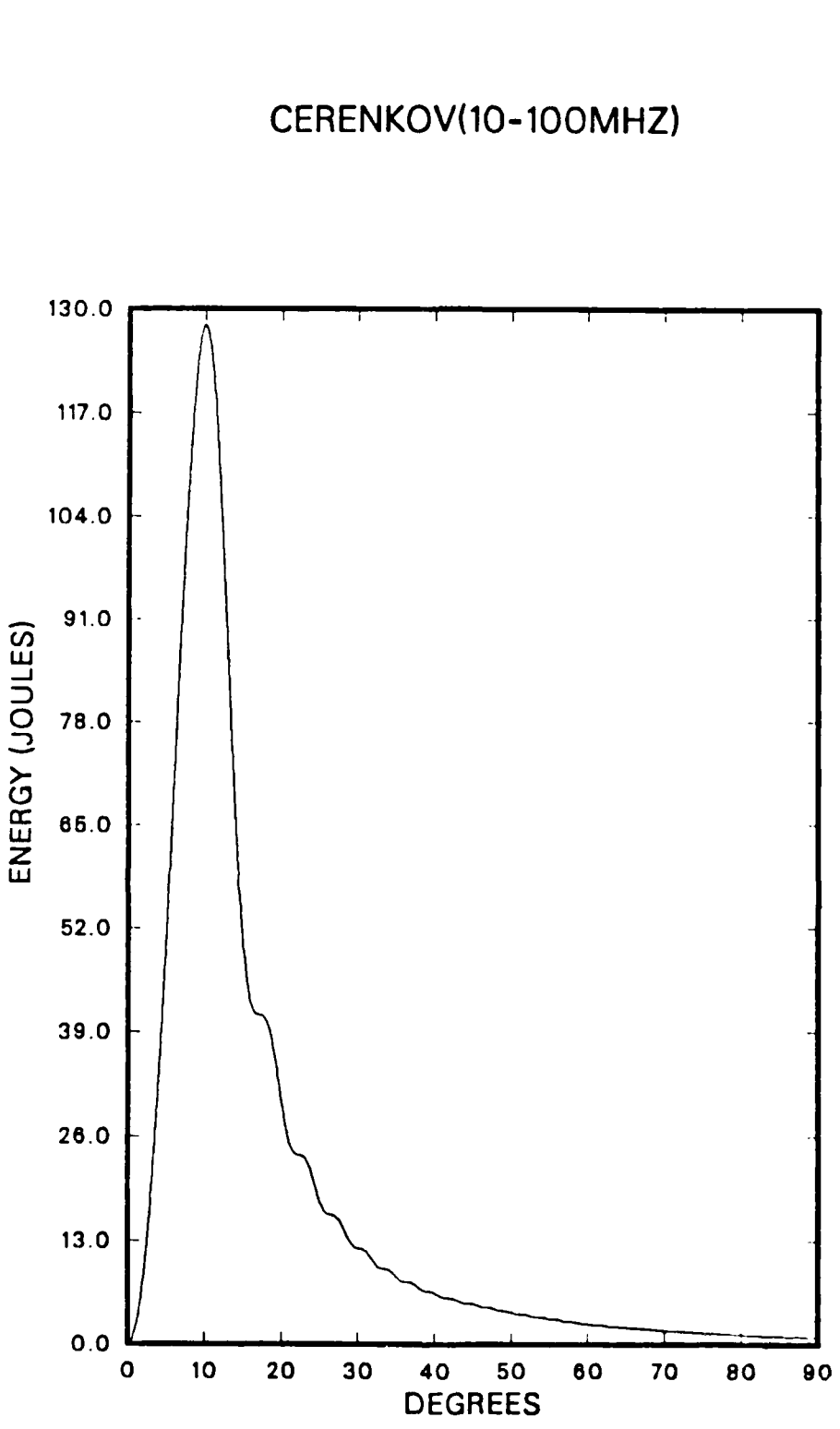

Figure 3.6 Energy per Unit Solid Angle, 10-100MHz., (Unity Form Factor).

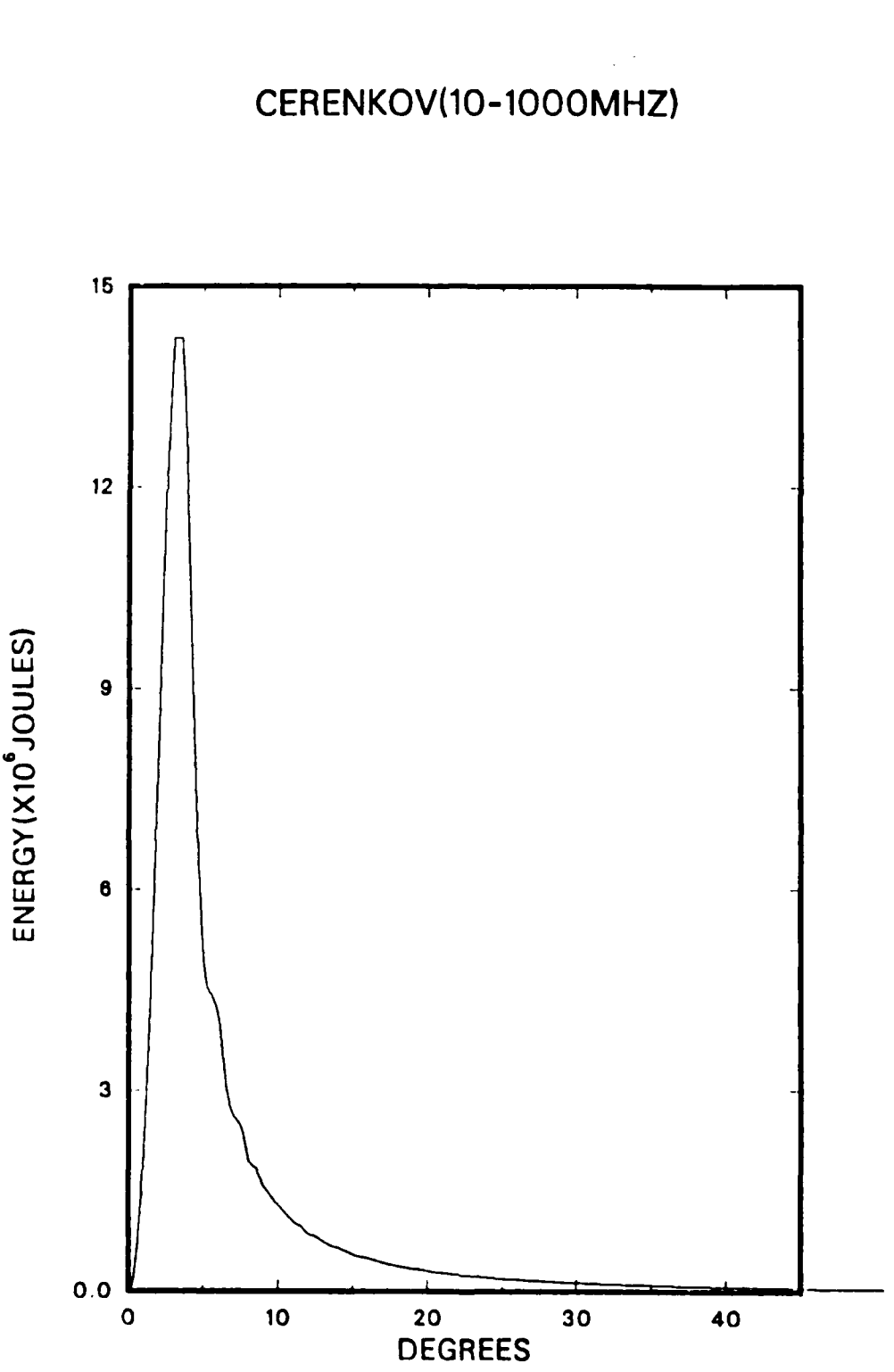

Figure 3.7 Energy per Unit Solid Angle, 10-1000MHz., (Unity Form Factor).

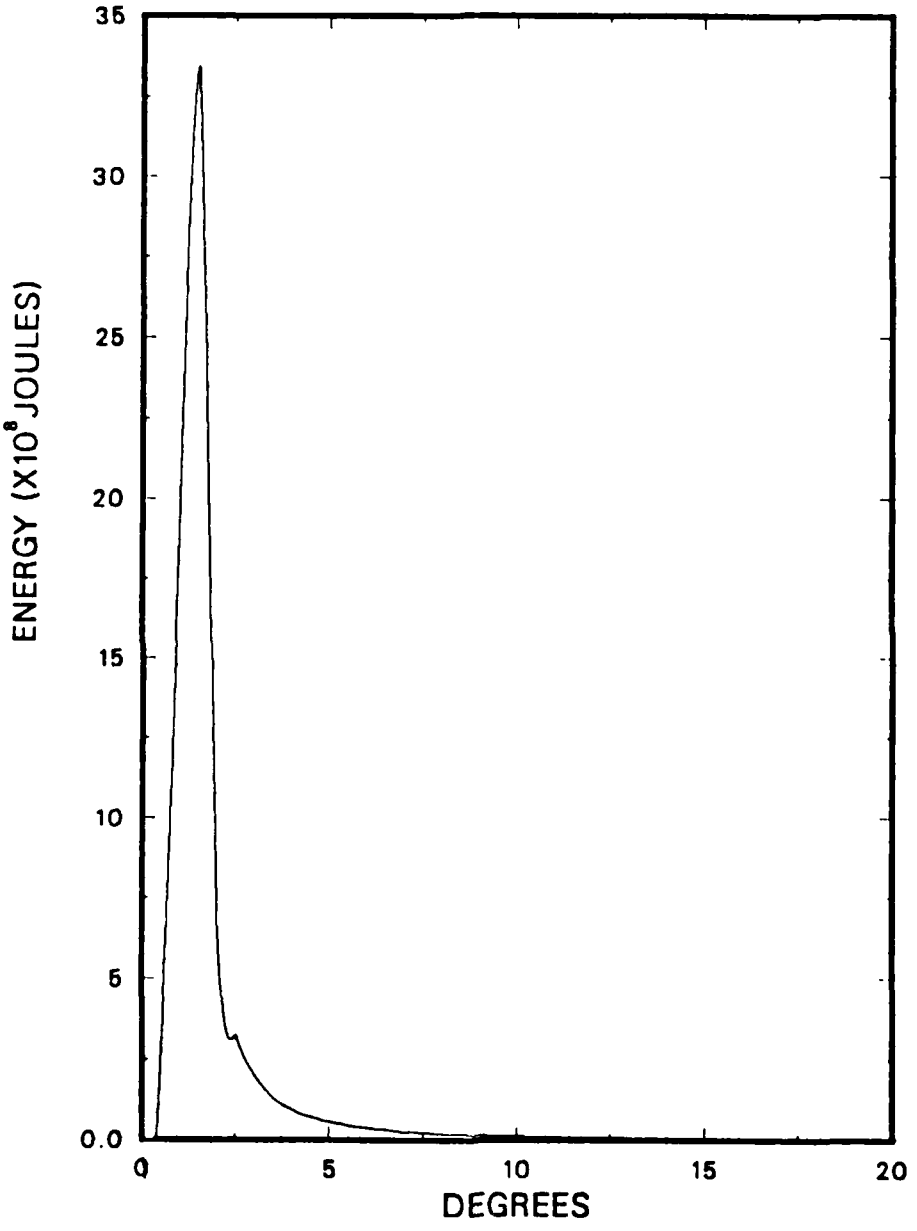

Figure 3.8 Energy per Unit Solid Angle, 10-10,000MHz., (Unity Form Factor).

$$\cos\alpha - \cos\gamma = -2\sin\{(\alpha/2)+(\gamma/2)\}\bullet\sin\{(\alpha/2)-(\gamma/2)\}. \qquad \text{(eqn 3.1)}$$

After a great deal of algebraic manipulation, it can be shown that the form factor will be of the form:

$$F(k) = \text{const}\bullet.\sin(\varepsilon)\bullet.\sin(\varphi), \qquad \text{(eqn 3.2)}$$

where $\varepsilon = \pi\cos\theta(d+b)\nu\ c$, and $\varphi = \pi\cos\theta(d-b)\nu\ c$.

For the trapezoidal bunch charge parameters used in this work, $c/(d-b)$ equates to a value of 200 MHz. and $c/(d+b)$ to a value of 18.2 MHz. Then, using the mean frequency of 100 MHz. found in Figure 3.13, one need only to equate each of the sin function arguments to integer values of π to mathematically determine the values of θ at which equation 3.2 will equal zero. Table 1 lists the values of θ at which the form factor will force zeroes in the energy equation.

TABLE 1
VALUES OF θ AT WHICH THE FORM FACTOR EQUALS ZERO.

$\sin\varepsilon = 0$	$\sin\varphi = 0$
$\theta_1 = 79.5°$.	undefined.
$\theta_2 = 68.7°$.	undefined.
$\theta_3 = 56.9°$.	undefined.
$\theta_4 = 43.3°$.	undefined.
$\theta_5 = 24.5°$.	undefined.

At the mean frequency of 100 MHz., $\sin\varphi = 0$ cannot be determined since it requires solving for an angle θ whose cos is greater than unity. However, by comparing the values of θ in column 1 of Table 1 to Figure 3.13, one sees a correlation of the null points to what can be considered the envelope of the output. It is clear then that the form factor acts as the modulator of the energy spectra of the Cerenkov radiation.

The "carrier wave" nulls can be determined in a similar manner by analyzing the diffraction function (eqn.2.8) found in equation 2.6. Equating u to integer values of π and solving for θ will provide all angles θ at which the energy output will be zero. Table 2 lists a sample of the results for which sinu equals zero. Again, comparing the values of θ in Table 2 to Figure 3.13 , one sees that the calculated nulls equate to those of the "carrier wave".

TABLE 2
VALUES OF θ AT WHICH SINU EQUALS ZERO.

sinu = 0.
$\theta_8 = 40.6°$.
$\theta_9 = 43.1°$.
$\theta_{10} = 45.6°$.
$\theta_{11} = 47.9°$.
$\theta_{12} = 50.2°$.
$\theta_{13} = 52.4°$.
$\theta_{14} = 54.6°$.
$\theta_{15} = 56.6°$.
$\theta_{16} = 58.7°$.
$\theta_{17} = 60.6°$.

Figures 3.14 and 3.15 are graphs of the Cerenkov energy output over the same narrowband frequency interval of 2 MHz., but at the higher frequency range of 499 to 501 MHz. Although some detail is lost compared to the outputs of Figures 3.12 and 3.13, the same analysis can be conducted to determine the null points of both the "carrier wave" and the modulating form factor. Tables 3 and 4 list the values of θ for each null point similar to those found for Figures 3.12 and 3.13. The range of θ was chosen so that a meaningful comparison could be made with the outputs of Figures 3.14 and 3.15.

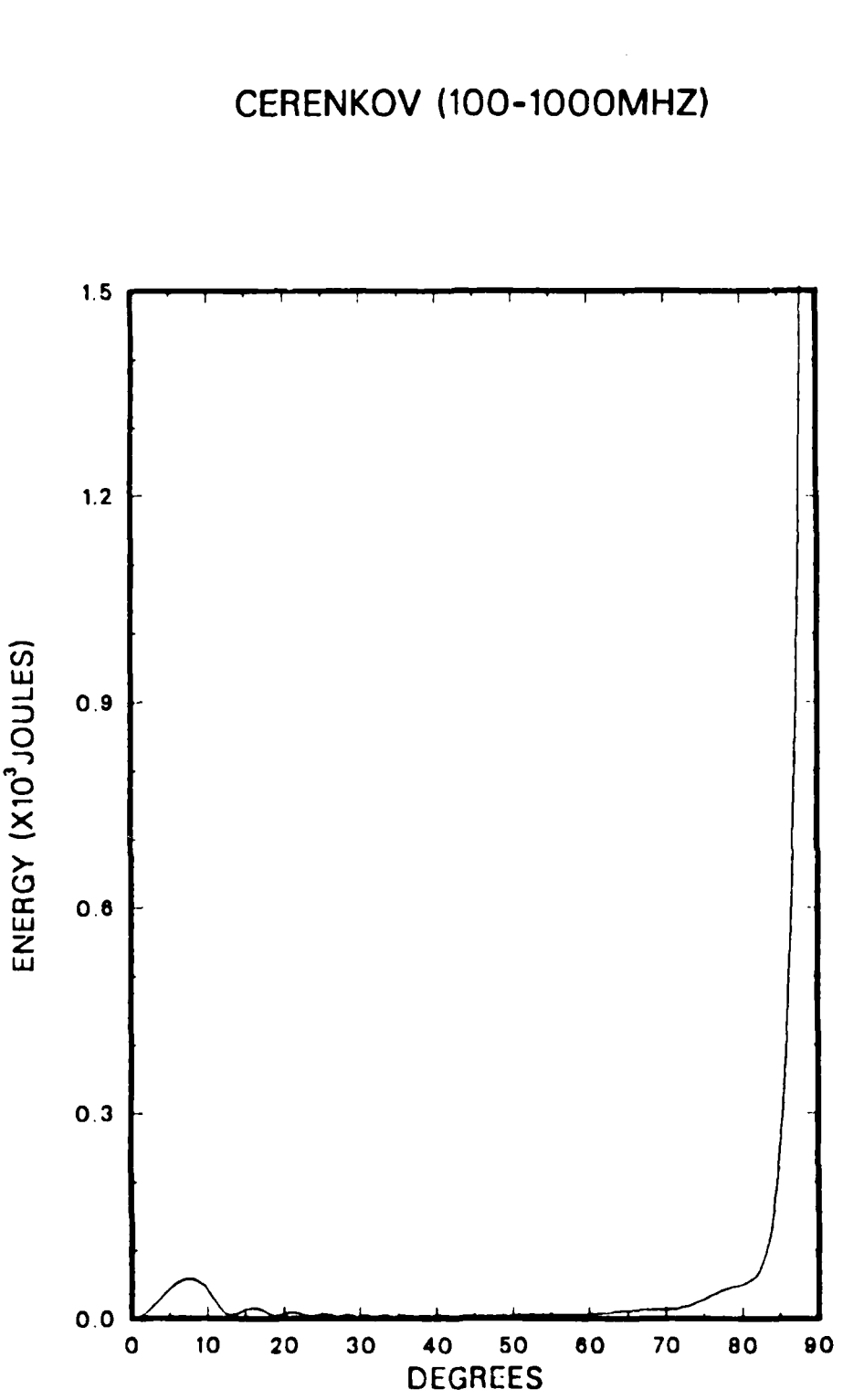

Figure 3.9 Energy per Unit Solid Angle, 100-1000MHz., (Trapezoidal Form Factor).

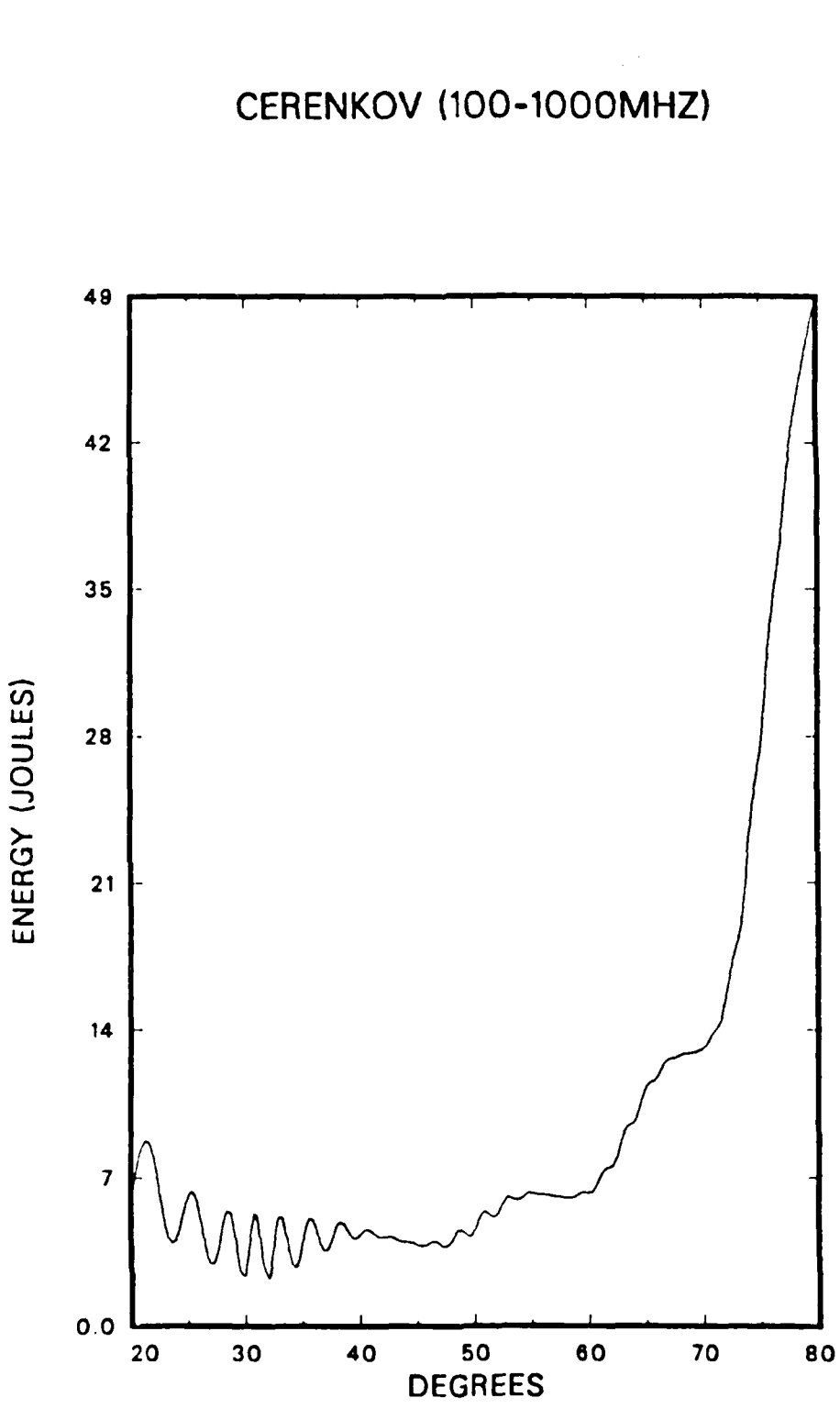

Figure 3.10 Energy per Unit Solid Angle, 100-1000MHz., (Trapezoidal Form Factor).

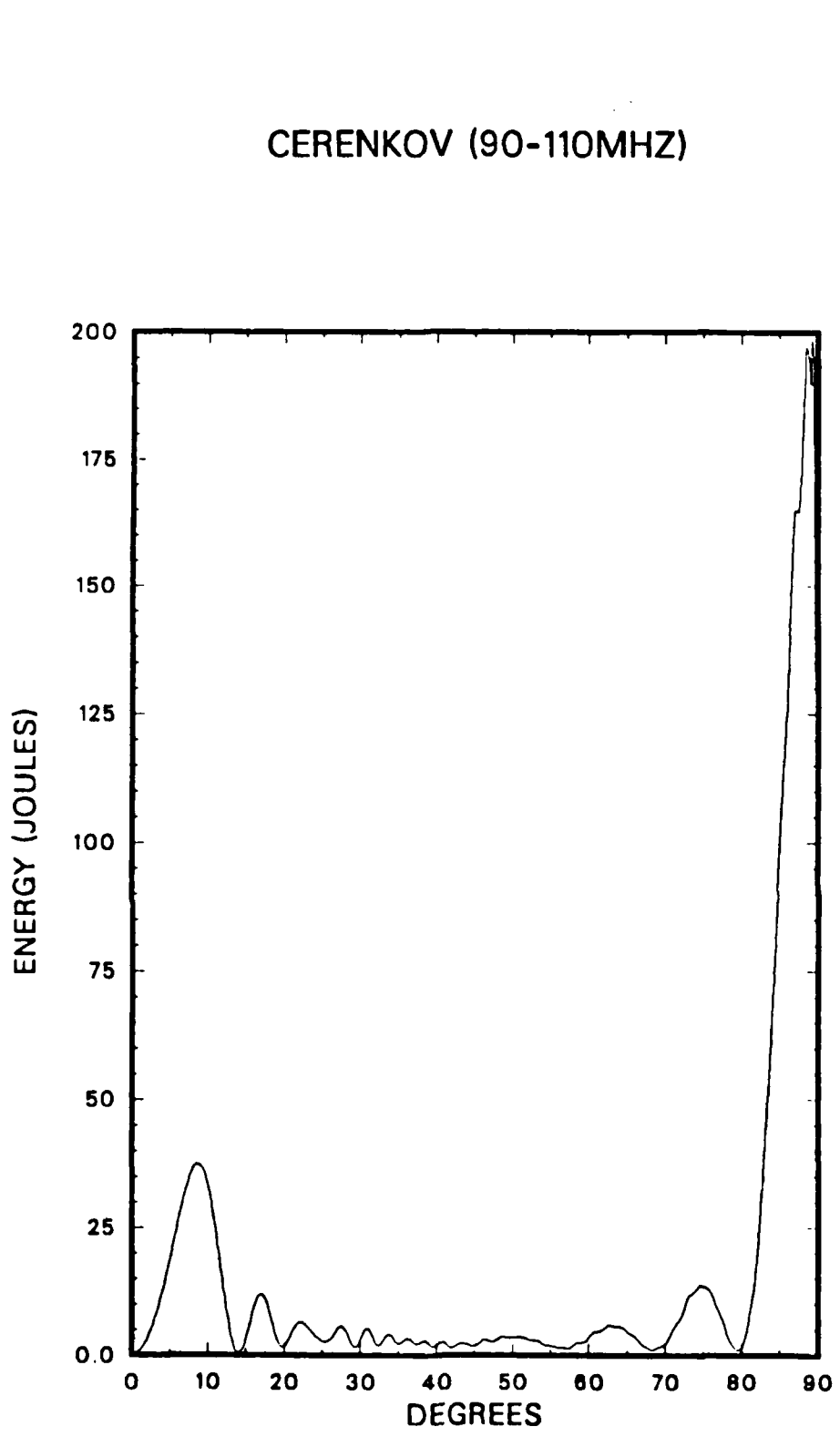

Figure 3.11 Energy per Unit Solid Angle, 90-110MHz., (Trapezoidal Form Factor).

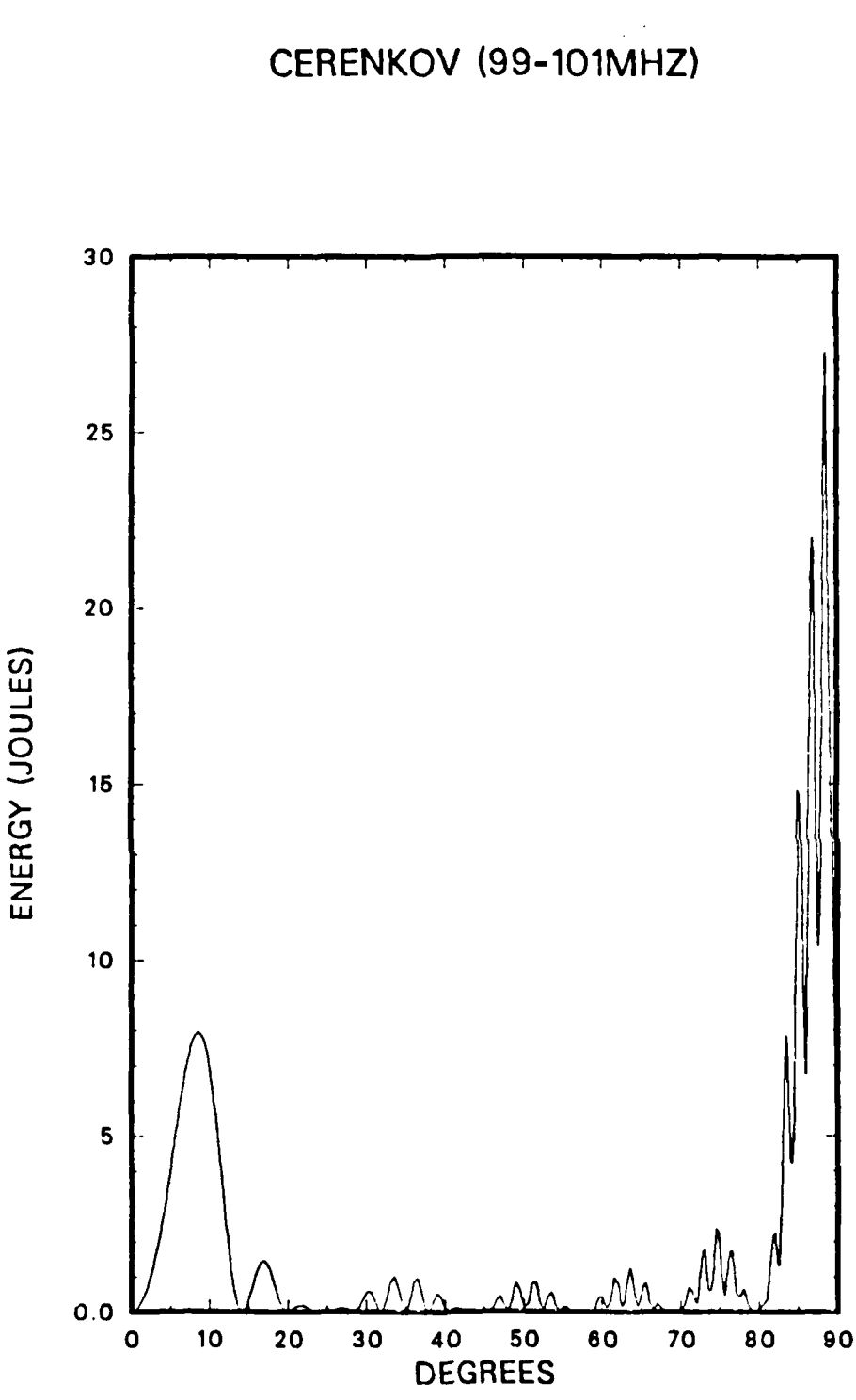

Figure 3.12 Energy per Unit Solid Angle, 99-101MHz., (Trapezoidal Form Factor).

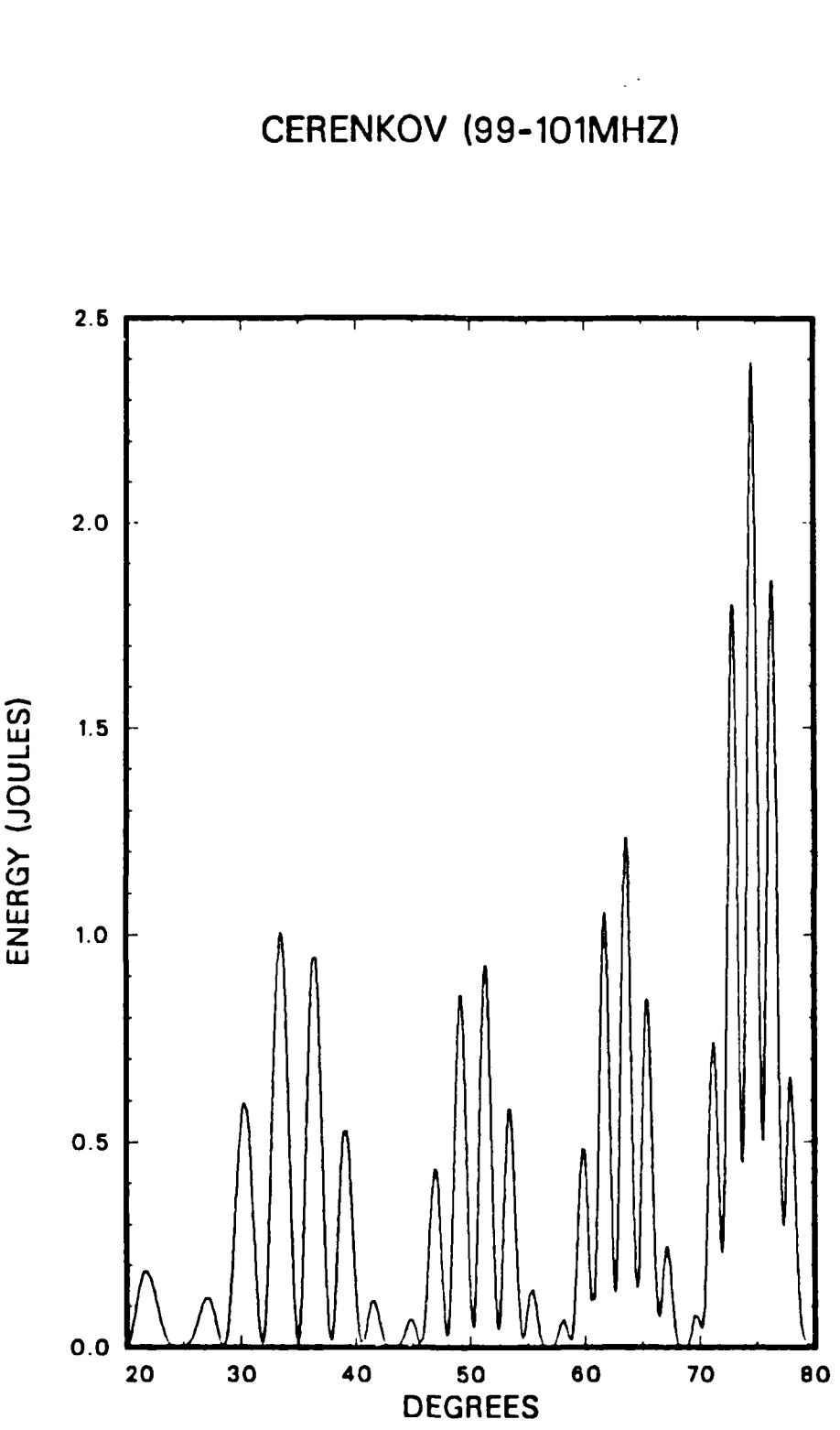

Figure 3.13 Energy per Unit Solid Angle, 99-101MHz., (Trapezoidal Form Factor).

TABLE 3

VALUES OF θ AT WHICH THE FORM FACTOR EQUALS ZERO.

$\sin\varepsilon = 0.$	$\sin\varphi = 0.$
$\theta_1 = 87.9°.$	$\theta_1 = 66.4°.$
$\theta_2 = 85.8°.$	$\theta_2 = 36.9°.$
$\theta_3 = 83.7°.$	undefined.
$\theta_4 = 81.6°.$	undefined.
$\theta_5 = 79.5°.$	undefined.
$\theta_6 = 77.4°.$	undefined.
$\theta_7 = 75.2°.$	undefined.

TABLE 4

VALUES OF θ AT WHICH SINU EQUALS ZERO.

$\sin u = 0.$
$\theta_{148} = 83.6°.$
$\theta_{149} = 83.9°.$
$\theta_{150} = 84.3°.$
$\theta_{151} = 84.6°.$
$\theta_{152} = 84.9°.$
$\theta_{153} = 85.3°.$
$\theta_{154} = 85.6°.$
$\theta_{155} = 85.9°.$

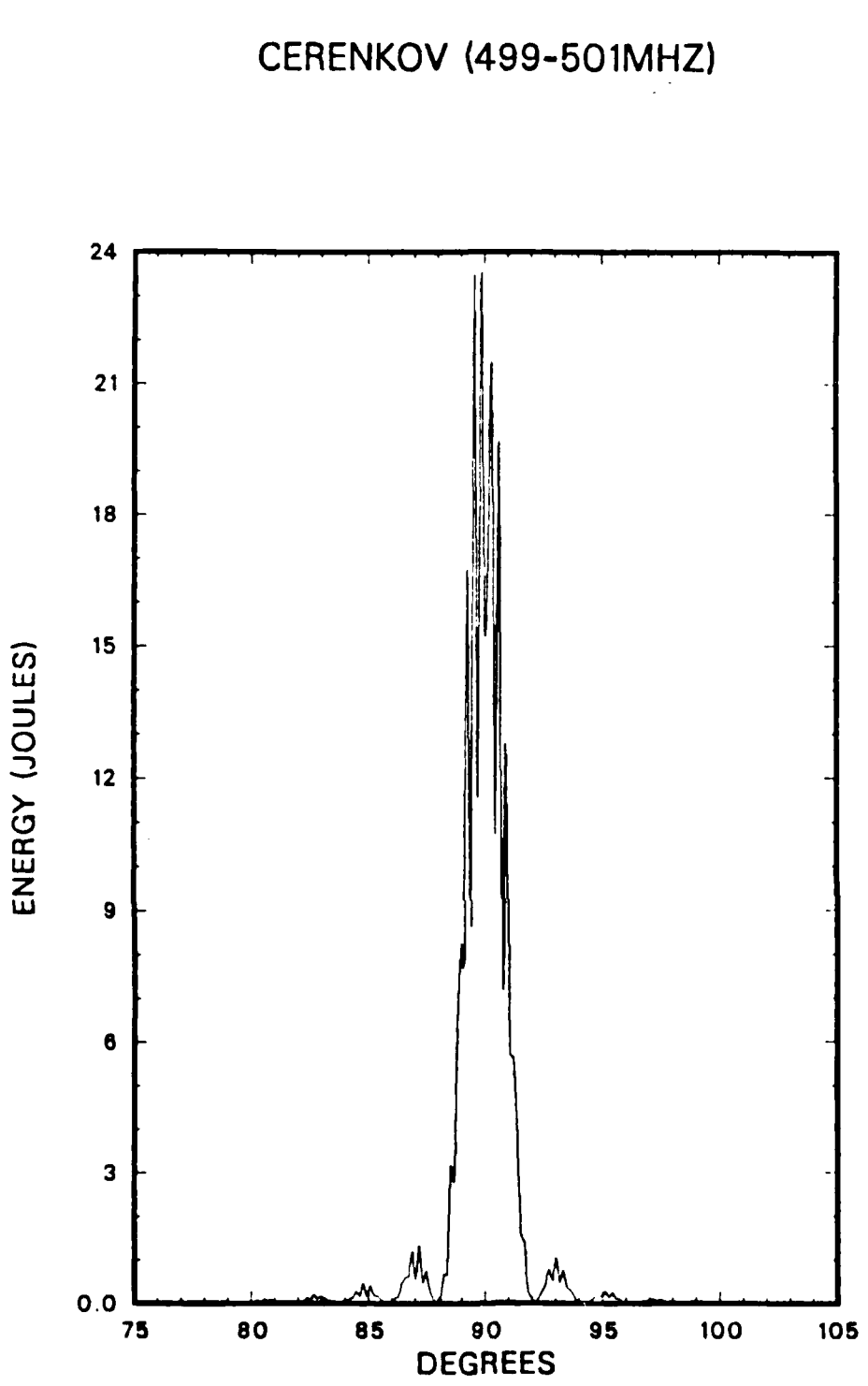

Figure 3.14 Energy per Unit Solid Angle, 499-501MHz., (Trapezoidal Form Factor).

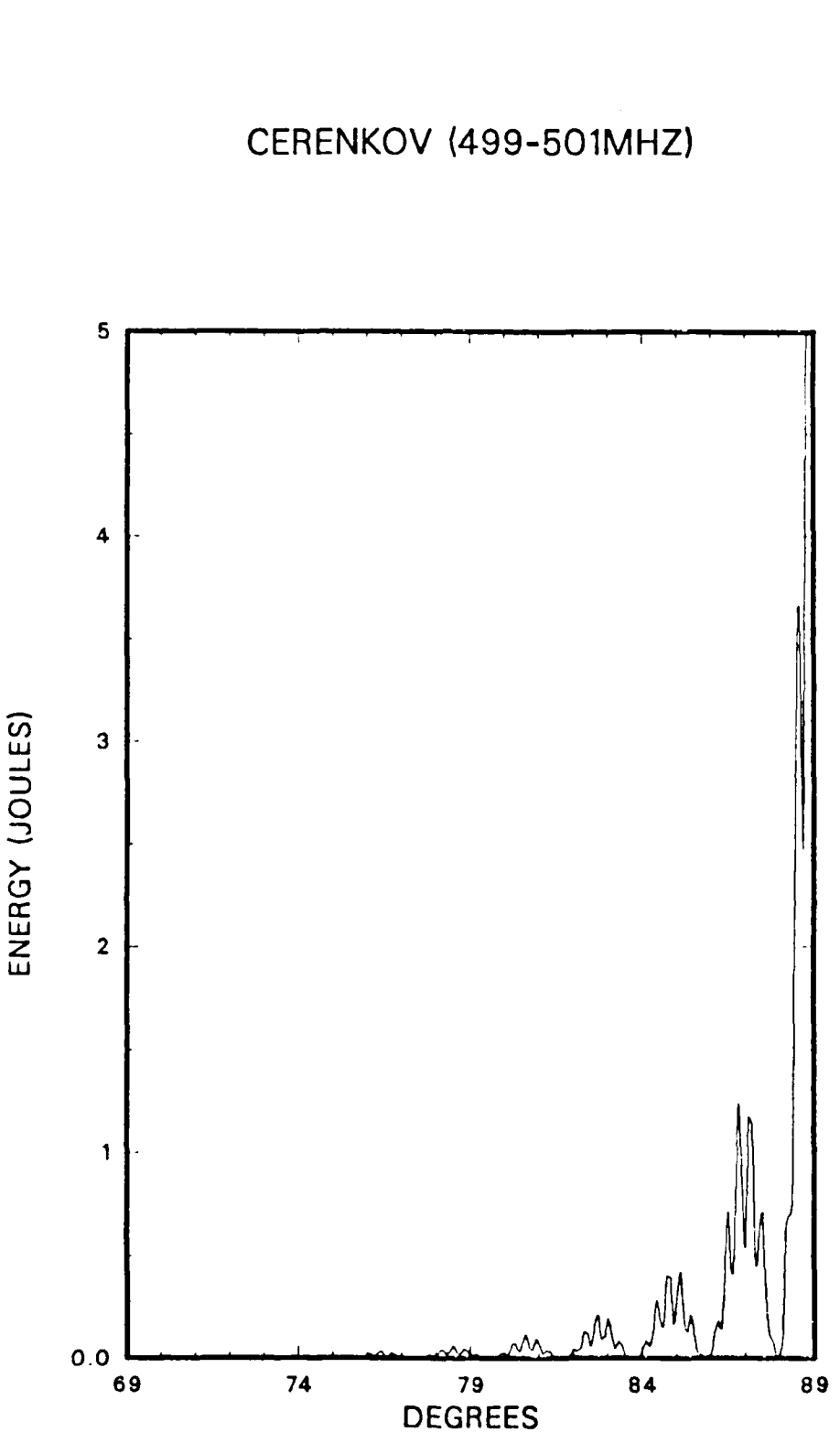

Figure 3.15 Energy per Unit Solid Angle, 499-501MHz., (Trapezoidal Form Factor).

IV. DISCUSSION

Figures 3.6 through 3.8 show that the energy radiated per unit solid angle from a charge distribution with unity form factor tends to be concentrated into an ever narrowing direction as the range of integration over frequency is increased. In the limit of all frequencies, the radiation is confined to the Cerenkov cone. The effect of including all frequencies is the same as allowing the beam path length to go to infinity, and the resulting radiation patterns are characteristic of that from a point charge.

The zeroes in the radiation patterns for trapezoidal charge distributions, Figures 3.9 through 3.15, are tabulated in Tables 1 through 4. Since the tables and figures are calculated from the same theory, they are, of course, in agreement. Tables 2 and 4 show the zeroes for the "carrier" oscillation which arises from the length of the electron beam path from source to detector. Tables 1 and 3 show the zeroes in the ε and φ oscillations resulting from the length (d+b) and rise time (d-b) respectively of an individual charge bunch. Both Tables show zeroes dictated by the length of the bunch charge. Only two zeroes from the pulse rise time occur; both at the higher frequency of measurement.

In the cases studied here, the bunch length (d+b) equals 16.5 meters and the pulse rise (d-b) equals 1.5 meters. At the measuring frequency of 100 MHz. the ratio of bunch length to wavelength is 5.5; large enough to resolve the details of the bunch size. Even at the higher frequency of 500 MHz. the ratio of pulse rise to wavelength is 2.5 and consequently the rise and fall of the pulse have little effect on the radiated output. [Ref. 5]

V. CONCLUSIONS AND RECOMMENDATIONS

After studying the figures depicting the radiated Cerenkov energy in this work, one could initially deduce that the use of narrowband detectors would be optimum for detecting radiation during any electron accelerator experiment. As shown and previously discussed, the information produced is more detailed when narrowband frequency ranges are used compared to wider band measurements. In particular, if one frequency band is considered as a function of angle, the calculated radiation energy has much detail as displayed in Figures 3.12 and 3.13 The structure depends on both the path length and bunch length, and, in principle, may yield information about these parameters. One must also consider the logistics of any experimental setup and any engineering problems involved to yield the maximum information.

For the broadband output with a unity formfactor, the energy output has a peak at the critical Cerenkov angle as expected. This output is typical of a point charge. However, since the nominal electron accelerator bunch charge output has a finite distribution, there is little information to be extracted from this particular output.

When the effect of the form factor is included, there exists a definite Cerenkov radiation peak perpendicular to the path the electron bunch is travelling. This phenomenon may be significant with respect to the optimum position at which the maximum energy produced by the radiation can be detected.

If a narrowband detection system is realistically feasible, it can be used to determine all nulls that arise in the energy equation due to the diffraction function and the form factor. Although narrowband detection will produce the most detailed output, its usefullness may be limited by the availability of equipment designed to discriminate the output within the desired frequency band limits.

In order to obtain significant information about the details of the charge distribution within a bunch, it will be necessary to perform experiments at frequencies such that the ratio of rise time to frequency is at least 5. For real beams, where the rise times are of the order of a few nanoseconds, this means that narrowband measurements must be performed at microwave frequencies.

To augment this research the following is recommended:

1. Analyze outputs with form factors other than trapezoidal, (i.e. rounded, triangular etc.).
2. Determine the optimum (higher) frequency bands for various frequency intervals at which useful information can be extracted.

APPENDIX
FORTRAN PROGRAM

```
C     PROGRAM TO COMPUTE THE ENERGY RADIATED PER UNIT SOLID ANGLE        TRI00010
C     OVER A SPECIFIC FREQUENCY RANGE
C
C    ********************************************************************
C    *       ERG ARRAY SIZE MUST CORRESPOND TO THE NUMBER OF            *
C    *                INCREMENTS OF THETA                               *
C    ********************************************************************
C
          DIMENSION ERG(1800)
C                                                                        TRI00020
C                                                                        TRI00030
            REAL ERG,COSANG,COSARG,COSGAR,KKONST,DEE,BEE
10        REAL FORFAC,EBEAM,LENGTH,KONST,C,GEE,TOP,BOT                   TRI00040
20        REAL ATHETA,RADFUN,PI,EREST,GAMMA,THETA,IND,MIDNU              TRI00050
30        REAL CONST,MU,CUE,TERG,TTERG,DNU,BNU,DEGINC,DATEND
          INTEGER IFORM,INCREM,DLOOP,D2LOOP,SELECT,NUMBER
          CHARACTER*1 RESPON,ANSW
C
C
C       ***EBEAM=BEAM ENERGY (MEV) ; FORFAC=FORM FACTOR (F(K))
C       ***ETA=BEAM LENGTH/WAVELENGTH ; BETA=VELOCITY/C(FOR MEDIUM)
C       ***GAMMA=RATIO OF BEAM ENERGY ELECTRON REST ENERGY
C       ***DIFFUN=DIFRACTION FUNCTION (I(U)) ; DTHETA=THETA(DEGREES)
C       ***THETA=THETA(RADIANS) ; LENGTH=LENGTH FROM SOURCE(METERS)
C       ***RADFUN=RADIATION FUNCTION; MIDNU=BEGINNING FREQUENCY
C       ***CUE=BUNCH CHARGE IN COULOMBS;EREST= ELECTRON REST ENERGY
C       ***ERG=ARRAY FOR STORING VALUES OF RADIATED ENERGY
C       ***                              FOR CUMULATIVE ANGLES THETA
C       ***DNU=FREQUENCY INTERVAL ;TERG=RADIATED ENERGY FOR A
C       ***                                  SPECIFIC ANGLE THETA
C
C
C     ***ASSIGNMENT OF CONSTANTS***
          CO=2.997925E8
          PI=3.14159
          EREST=.5117
          MU=1.2566E-6
C
C
          PRINT *,'THE INDEX OF REFRACTION (AIR) USED IS 1.000268'
          PRINT *,'DO YOU WANT A DIFFERENT VALUE?(Y/N)'
          READ (5,90)ANSW
90      FORMAT(A1)
              IF (ANSW .EQ.'N')THEN
                 IND=1.000268
                 GO TO 100
              ELSE
                 PRINT *,'SELECT THE INDEX OF REFRACTION (REAL)'
                 READ *,IND
              END IF
100     CONTINUE
C
C     DETERMINING THE SPEED OF LIGHT FOR THE MEDIUM
          C = CO/IND
C
          PRINT *,'ENTER BUNCH CHARGE (REAL) IN COULOMBS'
          READ *,CUE
260     CONTINUE
C
CCC   COMPUTATION OF CONSTANT (CALLED Q IN THESIS)
C
```

```
      CONST=MU*C*(CUE**2.)/(8.*(PI**2.))
      CALL EXCMS ('CLRSCRN')
C
C
      PRINT *,'ENTER THE DISTANCE FROM THE SOURCE (IN METERS)'
      PRINT *, 'THE RECEIVER WILL BE PLACED'
      READ *, LENGTH
      PRINT *, 'SELECT THE FORM FACTOR DESIRED:'
      PRINT *,'1=UNITY, 2=TRAPEZOID'
      READ *, IFORM
           IF (IFORM .EQ. 1)THEN
              FORFAC=1.0
              GO TO 290
           ELSE
             PRINT *,'ENTER THE TOP AND BASE VALUES (IN NANOSECONDS) FOR'
             PRINT *,'FOR THE CURRENT TRAPEZOID FUNCTION'
             READ *,TOP,BOT
C
C    THE NEXT 2 LINES CONVERT PULSE TIME TO DISTANCE
                   BEE = C*TOP/2.E9
                   DEE = C*BOT/2.E9
           END IF
290       CONTINUE
      CALL EXCMS ('CLRSCRN')
C
C   BEAM ENERGY SELECTION:USED TO CALCULATE BETA & GAMMA
C
      PRINT *, 'SELECT BEAM ENERGY:'
      PRINT *,'1=50 MEV ; 2= SELECT YOUR OWN'
      READ *,IBEAM
           IF(IBEAM .EQ. 1)THEN
              EBEAM=50.
              GO TO 300
           ELSE
              PRINT *,'INPUT THE DESIRED ELECTRON BEAM ENERGY IN MEV'
              PRINT *,'(INCLUDE DECIMAL POINT)'
              READ *,EBEAM
           END IF
300   CONTINUE
        GAMMA=EBEAM/EREST                                              TRI00100
        BETA=SQRT(1.-(1./GAMMA**2.))                                   TRI00110
      CALL EXCMS ('CLRSCRN')
C
C
      PRINT *, 'SELECT A FREQUENCY BAND TO BE SUMMED OVER AND THE'
      PRINT *,'INCREMENT IN MHZ:  1 =  A SUM OF FREQUENCIES'
      PRINT *,'FROM 10 MHZ TO 100 MHZ IN 10 MHZ INCREMENTS'
      PRINT *,'2 = SELECT YOUR OWN'
      READ *, INCREM
           IF (INCREM .EQ. 1)THEN
              BNU=10.E6
              DLOOP=9
              DNU=10.E6
              CALL EXCMS ('CLRSCRN')
              GO TO 400
           ELSE
              CALL EXCMS ('CLRSCRN')
CCCCCCCCCCCCCCCCCCCCCCCCCCCCCCCCCCCCCCCCCCCCCCCCCCCCCCCCCCCCCCCCCCCCCCCCCCCCCCC
C      CALL THE SUBROUTINE USED TO DEFINE FREQUENCY BAND OF INTEREST  C
C             AND THE INCREMENTAL STEPS FOR SUMMING                   C
CCCCCCCCCCCCCCCCCCCCCCCCCCCCCCCCCCCCCCCCCCCCCCCCCCCCCCCCCCCCCCCCCCCCCCCCCCCCCCC
              CALL FREQ(BNU,DNU,DLOOP)
           END IF
400   CONTINUE
C
C     OUTPUT GRAPH AXIS SELECTION
          PRINT *,'SELECT OUTPUT TYPE'
          PRINT *,'1=ENERGY VS. FREQUENCY FOR A SELECTED ANGLE THETA'
          PRINT *,'2=ENERGY(INTEGRATED OVER FREQ''S OF INTEREST) VS. THETA'
```

```
      PRINT *,'3=FORMFACTOR(F<K>) VS. FREQ. FOR A SELECTED ANGLE THETA'
      READ *,SELECT
      CALL EXCMS ('CLRSCRN')
           IF (SELECT .EQ. 1 .OR. SELECT .EQ. 3) THEN
           GO TO 470
           ELSE
           GO TO 450
           END IF
450   CONTINUE
      PRINT *, 'SELECT A RANGE FOR THETA AND THE INCREMENT AT WHICH'
      PRINT *, 'THE RADIATED ENERGY WILL BE CALCULATED'
      PRINT *, '1 = 0 TO 180 DEGREES IN ONE DEGREE INCREMENTS'
      PRINT *, '2 = SELECT YOUR OWN'
      READ *, NUMBER
           IF (NUMBER .EQ. 1)THEN
              D2LOOP=181
              DTHETA=0.0
              DEGINC=1
           ELSE
CCCCCCCCCCCCCCCCCCCCCCCCCCCCCCCCCCCCCCCCCCCCCCCCCCCCCCCCCCCCCCCCCCCCCCCCCCCCCCC
C        CALL THE SUBROUTINE USED TO DEFINE THE INCREMENTAL          C
C                      STEPS OF THETA                                C
CCCCCCCCCCCCCCCCCCCCCCCCCCCCCCCCCCCCCCCCCCCCCCCCCCCCCCCCCCCCCCCCCCCCCCCCCCCCCCC
              CALL DEGREE (DTHETA,DEGINC,D2LOOP)
           END IF
465   CONTINUE
           GO TO 500
470   PRINT *,'SELECT AN ANGLE (THETA) OF INTEREST.'
      READ *,DTHETA
           MIDNU = BNU
           TTERG = 0.0
           DLOOP=DLOOP+1
      GO TO 510
500   CONTINUE
        DO 600 K=1,D2LOOP                                          TRI00140
C
C    THIS OUTER LOOP WILL BE USED ONLY FOR OUTPUT TYPE 2
           TTERG=0.
           MIDNU= BNU+(DNU/2.)
510   CONTINUE
           THETA=DTHETA*PI/180.
           COSANG = COS(THETA)
           KONST = 2.*SIN(THETA)/((1./(IND*BETA))-COSANG)
           ATHETA = (LENGTH*PI/C)*((1./(IND*BETA))-COSANG)
C
C     THIS INNER LOOP IS USED FOR ALL 3 OUTPUT TYPES BY INCREMENTING
C          FREQUENCY OVER THE CHOSEN RANGE
              DO 550 J=1,DLOOP
                 IF(IFORM .EQ. 1)THEN
                    GO TO 515
                 ELSE
                    COSARG = 2.*BEE*PI/C
                    COSGAR = 2.*DEE*PI/C
                    KKONST = (C**2.)/(2.*(PI**2.)*((DEE**2.)-(BEE**2.)))
                    FORFAC=KKONST*(1./(MIDNU**2.))*(1./(ABS(COSANG)**2.))*
     D               (COS(COSARG*COSANG*MIDNU)-COS(COSGAR*COSANG*MIDNU))
                 END IF
515           CONTINUE
                 RADFUN=ABS(KONST*SIN(ATHETA*MIDNU)*FORFAC)                TRI00180
                 TERG=CONST*(RADFUN**2.)
                       IF (SELECT .EQ. 1) THEN
                          WRITE(21,520) MIDNU,TERG
520                FORMAT(2E10.5)
                       ELSE IF (SELECT .EQ. 3)THEN
                          WRITE (21,525) MIDNU,FORFAC
525                FORMAT(E10.5,E10.4)
                       ELSE
                          TTERG = TTERG + TERG
530             CONTINUE
```

```
                        END IF
                    MIDNU= MIDNU+DNU
550          CONTINUE                                                    TRI00200
           IF(SELECT .EQ. 1 .OR. SELECT .EQ. 3) THEN
           GO TO 600
           ELSE
           GO TO 555
           END IF
555    CONTINUE
            ERG(K)=TTERG* DNU
            GEE=ABS(KONST)**2.
            WRITE(21,560) DTHETA,ERG(K)                                TRI00190
560    FORMAT (2E10.5)
            DTHETA = DTHETA + DEGINC
600    CONTINUE
C      THE DATEND STATEMENT IS USED TO END THE DATA FILE
C           (NECESSARY IF USING DISSPLA GRAPHICS)
           DATEND=999.99
           WRITE(21,660) DATEND,DATEND
660    FORMAT (2F10.2)
           PRINT *, 'DO YOU WANT TO MAKE ANOTHER RUN?(Y/N)'
           READ (5,670)RESPON
670    FORMAT(A1)
           IF(RESPON.EQ.'Y') THEN
           CALL EXCMS ('CLRSCRN')
                GO TO 100
                ELSE
                GO TO 700
                END IF
700    CONTINUE
            STOP                                                       TRI00210
            END                                                        TRI00220
C
C
CCCCCCCCCCCCCCCCCCCCCCCCCCCCCCCCCCCCCCCCCCCCCCCCCCCCCCCCCCCCCCCCCCCCCCCCCCCCCCC
C
                        SUBROUTINE FREQ(BFREQ,DNU,DLOOP)
           REAL BFREQ,EFREQ,DIFF,DNU
           INTEGER DLOOP
           PRINT* ,'ENTER BEGINNING FREQUENCY IN MHZ(INCLUDE DECIMAL POINT)'
           READ* ,BFREQ
           BFREQ=BFREQ*1.E6
           PRINT* ,'ENTER ENDING FREQUENCY IN MHZ(INCLUDE DECIMAL POINT)'
           READ* ,EFREQ
           EFREQ=EFREQ*1.E6
           PRINT* ,'ENTER DESIRED INCREMENT IN MHZ(INCLUDE DECIMAL POINT)'
           READ* ,DNU
           DNU=DNU*1.E6
           DIFF=EFREQ-BFREQ
           DLOOP=INT(DIFF/DNU)
           RETURN
           END
C
C
CCCCCCCCCCCCCCCCCCCCCCCCCCCCCCCCCCCCCCCCCCCCCCCCCCCCCCCCCCCCCCCCCCCCCCCCCCCCCCC
C
                        SUBROUTINE DEGREE(BDEG,DEGINC,D2LOOP)
           REAL BDEG,EDEG,DEGINC,DIFFF
           INTEGER D2LOOP
           CALL EXCMS ('CLRSCRN')
           PRINT *,'ENTER STARTING AND ENDING ANGLES OF INTEREST(REAL)'
           READ *,BDEG,EDEG
           PRINT *, 'ENTER THE INCREMENTAL VALUE OF THETA(DEGREES) DESIRED.'
           READ *, DEGINC
           DIFFF = EDEG-BDEG
           D2LOOP =INT(DIFFF/DEGINC)+1
           RETURN
           END
```

LIST OF REFERENCES

1. Jelley, J.V., *Cerenkov Radiation*, Pergamon Press, 1958.

2. Neighbours, J.R., Buskirk, F.R., and Maruyama, X.K., *Cerenkov and sub-Cerenkov Radiation from a Charged Particle Beam*, paper accepted for publication by *Physical Review*.

3. Neighbours, J.R., "Personal Notes on Various Fourier Transformations," Naval Postgraduate School, Monterey, California.

4. Personal communication between Professor J.R. Neighbours, Naval Postgraduate School, Monterey, California, and the author, 19 March 1987.

5. Personal communication between Professor J.R. Neighbours, Naval Postgraduate School, Monterey, California, and the author, 24 March 1987.

BIBLIOGRAPHY

Buskirk, F.R., Neighbours, J.R.,"Cerenkov Radiation from Periodic Electron Bunches," *Physical Review*, v. 28, September 1983.

Buskirk, F.R., Neighbours, J.R., "Time Development of Cerenkov Radiation," *Physical Review*, v. 31, June 1985.

Buskirk, F.R., Neighbours, J.R., "Cerenkov Radiation and Electromagnetic Pulse Produced by Electron Beams Traversing a Finite Path in Air," *Physical Review*, v. 34, October 1986.

Milorad, Vujaklija, *Cerenkov Radiation from Periodic Electron Bunches for Finite Emission Length in Air*, M.S. Thesis, Naval Postgraduate School, Monterey, California, December 1984.

Stein, K.M., *Effects of Pulse Shaping on Cerenkov Radiation*, M.S.Thesis, Naval Postgraduate School, Monterey, California, June 1986.

INITIAL DISTRIBUTION LIST

		No. Copies
1.	Defense Technical Information Center Cameron Station Alexandria, Virginia 22304-6145	2
2.	Library, Code 0142 Naval Postgraduate School Monterey, California 93943-5002	2
3.	Professor J.R. Neighbours, Code 61Nb Department of Physics Naval Postgraduate School Monterey, California 93943-5000	6
4.	Professor F.R. Buskirk, Code 61Bs Department of Physics Naval Postgraduate School Monterey, California 93943-5000	3
5.	Professor K.E. Woehler, Code 61Wh Department of Physics Naval Postgraduate School Monterey, California 93943-5000	3
6.	LCDR Thomas M. Wilbur 9612 Chapel Hill Drive Burke, Virginia 22015	4
7.	Dr. Xavier K. Maruyama Bldg. 245, Room B-108 National Bureauof Standards Gaithersburg, Maryland 20899	1
8.	LCDR Johnny W. Green 5341 Dressagé Dr. Bonita, California 92002	1
9.	Mr. John D. Paulus 826 N. Meadowcroft Ave. Mt. Lebanon, Pennsylvania 15216	1

END

FEB.

1988

DTIC